This is to certify that the

dissertation entitled

STRUCTURAL ADAPTATIONS OF SUBMERSED VASCULAR PLANTS TO GAS EXCHANGE AND OXYGEN TRANSPORT

presented by

Jane Lenore Schuette

has been accepted towards fulfillment
of the requirements for

Ph.D. degree in Botany

Karen L Kempa
Major professor

Date August 9, 1990

STRUCTURAL ADAPTATIONS OF SUBMERSED VASCULAR PLANTS TO GAS EXCHANGE AND OXYGEN TRANSPORT

By

Jane Lenore Schuette

A DISSERTATION

Submitted to
Michigan State University
in partial fulfillment of the requirements
for the degree of

DOCTOR OF PHILOSOPHY

Department of Botany and Plant Pathology

1990

ABSTRACT

STRUCTURAL ADAPTATIONS OF SUBMERSED VASCULAR PLANTS TO GAS EXCHANGE AND OXYGEN TRANSPORT

By

Jane Lenore Schuette

Submersed vascular plants differ in their ability to transport and release photosynthetically-derived O_2 from their roots. This study examines the structural features of four morphologically distinct submersed species which may account for differences in O_2 transport known to exist between them. The high transport potential of *Lobelia* may be due to a thick cuticle which promotes lacunar storage of O_2, a large lacunar volume and a short continuous pathway between leaves and roots. Species with lower transport potentials such as *Elodea*, *Myriophyllum* and *Potamogeton* are characterized by leaves with thin cuticles, smaller lacunar volumes and long transport pathways. A hypodermis may protect buried roots from reduced phytotoxins and retard O_2 loss.

The lacunar system formed a continuous pathway for gas transport throughout the length of the stem, although constricted at the nodes by perforated diaphragms. Gas transport studies showed that diaphragms provide little resistance to diffusion, but considerable resistance to mass flow. Diffusive resistances measured closely approximated those predicted by Fick's first law. As the porosity of the stem increased from *Elodea*, *Myriophyllum* to *Potamogeton*, resistance to diffusion decreased, thus suggesting an increasing ability to transport O_2 to the roots among these species. The

results suggest that the O_2 transport requirements of the species examined may, during periods of active photosynthesis, be satisfied by diffusion alone. These findings also suggest that plants with high internal resistances could not transport enough O_2 by diffusion alone to support a large root biomass.

Measured resistances to mass flow approximated those predicted by Hagen-Poiseuille equation. Mass flow could occur in these plants under small pressure differentials, since measured resistances were, with the exception of *Elodea*, quite low. The significance of mass flow to O_2 transport could not be determined.

A model is proposed which describes the distribution of rooted submersed vascular plants in lakes with increasing sediment O_2 demand. It suggests that species distributed along this gradient may be characterized by a decrease in lacunar development, relative root production and their dependency on the sediments as a site of nutrient uptake.

ACKNOWLEDGMENTS

I gratefully acknowledge the encouragement and support from my advisor, Dr. Karen Klomparens and the technical assistance of everyone at the Center for Electron Optics. It has also been a privilege to be associated with the Kellogg Biological Station and I am especially grateful to Dr. Mike Klug for his invitation as well as his inspiration. I would particularly like to thank Dr. Ken Poff for his advice, encouragement and continued interest in my research and career. I would also like to acknowledge the fruitful discussions with committee member Dr. Frank Ewers and with friends and colleagues, Drs. Fred Payne, Rick Carlton, Mike Kaufman and Rich Losee. Finally, I would like to thank my family, friends and aerobics for their support throughout this endeavor.

TABLE OF CONTENTS

LIST OF TABLES

LIST OF FIGURES

INTRODUCTION

Submersed vascular plants are exposed to two potential sources of nutrients- those dissolved in the surrounding water and those in O_2 deficient sediments. Roots buried in these sediments require an alternate source of O_2. O_2 transport from the shoots to the roots is necessary not only to satisfy their respiratory demands but also, upon release, to support an oxidized rhizosphere within the sediments (Sculthorpe, 1967; Hutchinson, 1975; Wetzel, 1975). The lacunar system is a network of intercellular gas spaces found in leaves, stems and roots of aquatic vascular plants which performs two important functions in this process. It serves as a reservoir for O_2 storage within the plant and provides a pathway for O_2 transport throughout the plant body.

In a diurnal study, Hartman and Brown (1967) showed that O_2 produced during photosynthesis accumulates within the lacunar atmosphere of submersed plants before it is released to the surrounding water. O_2 stored within the lacunar system of the shoots can be transported to rhizomes and roots and can also be released to the sediments (Oremland and Taylor, 1977). Release of O_2 from the roots of submersed plants is known to be much greater in the light than in the dark (Sand-Jensen et al., 1982; Sand-Jensen and Prahl, 1982; Carpenter et al., 1983; Smith et al., 1984; Kemp and Murray, 1986), thus implying that most of the O_2 transported to the roots is of direct photosynthetic origin. It is generally accepted that, on a diurnal basis, respiration in the

rhizomes and roots is supported primarily by the photosynthetic activity of the shoots (Sculthorpe, 1967; Wetzel, 1975; Smith et al., 1984).

Submersed macrophytes have been shown to differ in their lacunar storage and transport potentials. Among eight species investigated, Sand-Jensen et al. (1982) found marked differences in the amount of O_2 released by the roots relative to that released by the shoots. In the isoetid species examined, *Lobelia dortmanna*, the amount of O_2 released by the roots as a percentage of total shoot plus root release was high (100%). This value was low (1-4%) in the other species investigated where release across the shoots was favored. These results suggest that submersed vascular plants may possess different morphological and structural features which influence the exchange of gases between the plant and its surroundings.

The exchange of O_2 between the lacunar atmosphere and surrounding water can most simply be described by Fick's first law of diffusion (Armstrong, 1979):

$$\text{Flux} = O_2 \text{ Gradient} \times \frac{\text{Surface area}}{\text{Resistance}}$$

Assuming a constant O_2 gradient, the rate of flux across either the shoots or the roots is thus determined by the surface area and the resistance of the tissue to diffusion. From a morphological/anatomical standpoint, high release rates of O_2 across the roots may be favored by a combination of the following features:

1) a large surface area of shoots relative to roots

2) a high resistance across leaves

3) a low resistance across roots

4) a lacunar pathway of low resistance.

Release of O_2 across the shoots may be facilitated by:

1) a large surface area of roots relative to shoots

2) a low resistance across leaves

3) a high resistance across roots

4) a lacunar pathway of high resistance.

Objectives

The purpose of this research was to evaluate differences in the lacunar O_2 storage and transport potentials of submersed vascular plants on the basis of their anatomical and/or structural features. If a primary function of the lacunar system is to transport O_2 to the roots, one may expect to find that differences between submersed species in their ability to transport O_2 may be related to the relative amount of roots that species typically produces. Four submersed species with known differences in gas exchange characteristics, as well as contrasting morphologies, root:shoot ratios and distributional preferences, have been selected for examination to determine the following:

1). What is the general anatomy of the leaves and what features do they possess that may influence gas exchange?

2). What is the general anatomy of the lacunar system of the selected species and what, if any, are the relative differences in the extent of lacunar development?

3). What is the general anatomy of the roots and what features do they possess that may influence gas exchange?

4). What influence does the structure of the lacunar system have on mechanisms of gas transport?

Each objective is presented in a separate chapter. These chapters are organized in the sequence of events in which O_2 transport occurs, namely: lacunar storage of O_2 in leaves (Chapter I); long-distance transport of O_2 from the leaves to the roots (Chapter II); and release of O_2 from the roots (Chapter III). In the final chapter (Chapter IV), the influence of lacunar structure on the ability of submersed plants to transport O_2 is examined. These chapters are then synthesized in a final summary which examines the physiological and ecological significance of whole plant strategies to gas exchange.

MATERIALS AND METHODS

Species examined.

The species selected for anatomical and ultrastructural examination include *Elodea canadensis*, *Myriophyllum heterophyllum*, *Potamogeton praelongus* and *Lobelia dortmanna*. Hereafter these species are refered to by their generic names, unless it is necessary to distinguish them from other members of the same genus.

Elodea canadensis

Elodea canadensis Rich (Hydrocharitaceae; Monocotyledoneae), a common aquatic species, is often abundant in small ponds and reservoirs, forming either floating mats or dense stands which are sparsely rooted to the sediments (Hutchinson, 1975). It consists of a segmented stem which is produced by an apical meristem in a series of nodes and internodes. Internodes are cylindrical in shape, 0.5-2.0 mm in diameter, and decrease both in length and width towards the shoot apex. Leaves, roots and branches emanate from the stem as nodal outgrowths (Dale, 1957a). Leaves are linear-lanceolate in shape, 6-12 mm long, and possess a single midvein. They are sessile, only slightly constricted at the base and are found most often in whorls of 3. An underground rhizome is not produced; roots arise adventitiously from the nodes of the stem and account for less than 3% of the total plant biomass (Borutskii, 1950 in Westlake, 1965).

They are unbranched, often over 20 cm in length and less than 1 mm in diameter. The mature plant commonly produces both sediment and water roots. Water roots are light green in color and are devoid of root hairs; those penetrating the sediments are white and develop an abundant supply of root hairs (Cormack, 1937).

Myriophyllum heterophyllum

Myriophyllum heterophyllum Michx. (Haloragaceae; Dicotyledoneae), commonly called water-milfoil, is a perennial aquatic which often exhibits a heterophyllous condition. This species has recently become abundant in New England where it grows aggressively in ponds, lakes and streams of low alkalinity. To the west, it typically is found in waters of high alkalinity (Crow and Helquist, 1983). At maturity, it is characterized by a rhizotomatous growth habit. New upright stems arise from overwintering buds which develop either at the base of old stems or on the rhizome. Stems are long and flexuous and are divided into nodal and internodal regions. Internodes are cylindrical in shape, range from 1-4 mm in diameter, and decrease both in length and width towards the shoot apex. Leaves are found in groups of 4 at the node. Submersed leaves are highly dissected and pinnately compound with usually 7-10 pairs of fine, nearly cylindrical leaflets that are arranged flat on the rachis, tapering in length towards the apex of the leaf. They typically measure less than 1 cm in length and 0.5 mm in diameter. The rhizome is usually short and compact, producing slender and unbranched adventitious roots at the nodes. Both the roots and rhizome are buried in the sediments and, in related members of this genus, account for roughly 10% of the total plant biomass (Nicholson and Best, 1974; Chambers and Kalff, 1985). The roots commonly measure up to 20 cm or more in length and less than 1 mm in diameter.

Young buried roots appear silver-grey in color and become dark brown to black at maturity. Water roots, light green in color, are often produced at nodes of the stem and are positioned well above the sediment surface.

Potamogeton praelongus

Potamogeton praelongus Wulfen (Potamogetonacceae; Monocotyledoneae) is a common deep water annual of temperate lakes (Spence and Crystal, 1970). It consists of a buried horizontal rhizome system which is segmented and produces long upright leafy stems and numerous adventitious roots at the nodes. The stem is differentiated into nodes and internodes. Internodes are cylindrical in shape, range from 1.5-4 mm in diameter and decrease in both length and width towards the shoot apex. Leaves are produced by an apical meristem in alternate arrangement at the nodes. They are oblong-ovate in shape and commonly measure 10-15 cm long and 2 cm at the widest point. The venation is characterized by a wide (1-2 cm) central midvein with 5-8 minor midveins and fibrous ribs on either side. The leaves are sessile and subcordate. Fibrous stipules are formed in the leaf axils. The root/rhizome system is extensive; in related members of this genus, it accounts for 12% (Nicholson and Best, 1974) to 40-50% (Ozimek et al., 1974) of the total plant biomass. Both roots and rhizome are cream in color and mottled with reddish-orange spots. The roots are slender and unbranched, often measuring 10 cm or more in length and less than 0.5 mm in diameter. Root hairs are usually present (Shannon, 1953).

Lobelia dortmanna

Lobelia dortmanna L. (Lobeliaceae; Dicotyledoneae) is a small isoetid species that is commonly rooted in shallow sandy areas of soft-water oligotrophic lakes (Moyle, 1945). It is a relatively slow growing perennial which overwinters as an evergreen, undergoing only small seasonal fluctuations in total plant biomass (Moeller, 1978). Leaves are stiff and tubular to strap-like in shape and usually measure less than 5 cm long and 1-3 mm wide. They are produced close together in a basal rosette and are directly attached to a short (1-3 cm long), compact and unsegmented stem. The stem is buried in the sediments and produces an abundant root system in close proximity to the leaves. Usually 2-4 roots are associated with each leaf and are inserted into the stem on each side of the leaf at its base. Roots are cream in color, unbranched, and typically less than 10 cm long and 1 mm in diameter. Root hairs are usually not produced (Søndergaard and Laegaard, 1977). The roots and stem collectively account for 50-65% of the total plant biomass (Sand-Jensen and Søndergaard, 1979).

Collection of plant material for microscopical examination.

Plants of *Elodea*, growing loosely attached to the sediment, were collected with a rake from shallow water (1-2 m) in the outdoor experimental ponds at the Limnological Research Laboratory and from ponds at the Waste Water Research Facility of Michigan State University, Ingham County, Michigan.

Submersed plants of *Myriophyllum* and *Potamogeton*, rooted in calcareous sediments, were collected either by hand or with a rake in shallow (1-4 m) water at Lawrence Lake, Barry County, Michigan.

Plants of *Lobelia*, growing submersed (1-2 m) in coarse sandy sediments were collected by hand in the St. Mary's River, Chippewa County, Michigan. At the time of collection, plants were gently freed from the sediments and transported to shore in plastic bags containing lake water. Samples were prepared for microscopical examination within 1 hour after collection. Despite care taken in handling, much of the loosely attached periphytic community was dislodged from the plant, this study therefore examines only the portion securely attached to the plant surface.

3. Tissues selected for microscopical examination.

Samples for anatomical observations were taken from leaves, roots and stems, as well as the junctions of these organs. For ultrastructral examination, samples were taken from the midsection of young, fully matured expanded leaf blades and young, fully mature healthy roots.

Tissue preparation and microscopical examination.

For transmission electron microscopy (TEM), tissues were fixed with cold 4% gluteraldehyde in 0.1 M phosphate buffer at pH 7.2 for 2-3 hours, washed twice in same buffer, post-fixed in 1% osmium tetroxide either for 1.5-2 hours at room temperature or overnight at 4°C, dehydrated in a graded ethanol series (25%, 50%, 75%, 95%, 100%), followed by increasing proportions of acetone in absolute ethanol (1:2, 2:1 and absolute) and embedded in a 1:1 mixture of Spurr's (1964) and Mollenhauer's (1969) epoxy resin. At various steps in the procedure, a vacuum was drawn to remove gases from gas spaces within the tissue and to facilitate infiltration of reagents and resin. Polymerization was for a minimum of 48 hours at 60°C. Ultrathin sections were cut with glass and diamond

knives and stretched with xylene. Gold to silver sections were picked up on copper mesh grids, stained with uranyl acetate and lead citrate (Reynolds, 1963) and examined in a Philips 201 Electron Microscope at 60 and 80 kV.

For scanning electron microscopy (SEM), tissues were typically fixed and dehydrated as above. Post-fixation in osmium was eliminated in some samples. All samples were dried via liquid CO_2, mounted on aluminum stubs, coated with gold and examined in either an ISI Super-III or JEOL 35C Electron Microscope.

For light microscopy, tissues prepared for TEM were sectioned at 1-2 μm, heat fixed in 5% acetone to glass microscope slides, and stained with toluidine blue (Feder and O'Brien, 1968). Samples were also fixed in formalin acetic acid (FAA), embedded in paraplast, sectioned on a rotary microtome at 10-20 μm, and double stained with safranin and fast green as described by Johansen (1940).

Measurement of Resistance.

Sampler

Resistance estimates were determined using a simple sampler consisting of two 5 ml glass pipets capped with serum stoppers. Stems were inserted into tygon-tubing collars fitted around the dispensing end of the pipet and were sealed with vaseline to prevent flooding. The entire sampler was submersed in a water bath. Care was taken to insure proper fit. Improper fit resulted in either damage to the stem or flooding of the sampler. Measurements were discarded when these problems were evident. Estimates of resistance to both diffusion and mass flow were made on the same stem section without removal from the sampler.

Diffusion

Resistance to diffusion was determined by constructing a standard curve (Appendix I). Sections of glass capillary tubing of known resistance were inserted into the sampler. Injections of tracer gas (0.1 ml of 10% CH_4, 90% Ar) were made into one end to the sampler. After 2 hours, a 0.1 ml gas sample was extracted from the opposite end. The CH_4 present in the sample was determined using a Varian gas chromatograph equipped with a Porapak N column and operated at 50°C. The CH_4 present was expressed as a percent relative to control samplers with no added resistance which were run concurrently. Typically each run consisted of 6 samplers and 4 controls. Regression analysis was performed on these data and a linear equation derived which describes percent transported as a function of resistance (Appendix I).

Transport values were determined similarly for samplers containing stem tissues. Estimates of diffusive resistance (R, s cm^{-3}) obtained were divided by the length of stem section and are expressed as resistance per cm stem.

Mass Flow

Mass flow estimates were made prior to diffusion estimates. Gas tight, S-shaped glass ports were connected to the submersed end of the sampler via 22 gauge needles. The total volume of the mass flow sampler was 38.5 ml. Injections of 0.1 ml room air were made through a serum stopper at the emergent end of one port. A Validyne pressure transducer was connected to a similar port at the opposite end of the pipet sampler. The change in pressure within the sampler with time after injection was displayed on a chart recorder. Both the time ($t_{.5}$) required to reach half the final equilibrated pressure (.5ΔP) and the pressure at one half ΔP were determined. The

amount of gas that passed through the stem at ΔP was calculated and the volumetric flow rate (F, $cm^3\ s^{-1}$) determined by dividing this amount by $t_{.5}$. Resistance (r, kPA s cm^{-3}) was estimated using Hagen-Poiseuille equation ($r=\Delta P/F$) and represents the mean of 3 individual runs. Estimates are expressed as resistance per cm stem.

Image Analysis

The length and diameter of stem sections were measured with a calipers and the number of nodes and/or visible diaphragms were recorded.

For image analysis of stem gas space, freehand sections were cut with a razor blade, mounted on glass slides and video-taped. Images of sections were divided into quarters, using the center of the vascular cylinder as the midpoint. Images were analyzed for radius, porosity, gas sapce area, lacunar size and number using a Microscience Image Analysis System. Each estimate is based on the mean of 3 measurements. For image analysis of nodes and diaphragms, stem sections were fixed for SEM in 1% gluteraldehyde and processed as above.

Porosity values were also estimated from 35 mm photographs taken from thick sections of stems and roots embedded for TEM. Gas spaces were delineated on each photograph. The area occupied by gas space and by epidermal, cortical and vascular tissues was determined with a planimeter. These areas are expressed as percent cross-sectional area and represent the mean of 3 measurements.

CHAPTER I

LEAF ANATOMY: STRUCTURAL RESISTANCES TO GAS EXCHANGE

INTRODUCTION

Gases diffuse 2 or 3 orders of magnitude slower in water than in air (Leyton, 1975). In leaves of many submersed species, this physical constraint has resulted in the adaptation of several morphological and anatomical features which facilitate the exchange of gases between the leaf and the surrounding water (Arber, 1920; Sculthorpe, 1967). Leaves of these plants tend to be long and thin or highly dissected in shape, thus maximizing the surface area for absorption. Stomates are absent, gas exchange is thought to occur across the entire leaf surface. The leaves are often only a few cell layers thick so nearly every cell is in direct contact with the bulk water phase. Epidermal cells commonly contain chloroplasts and are covered by a thin cuticle. These features decrease the path length for diffusion of gases as well as the resistance to gas flow across the leaf surface.

Gas spaces are also present in the leaves of many submersed species and can facilitate the rapid internal diffusion and storage of gases (Hough, 1979; Søndergaard, 1979; Søndergaard and Wetzel, 1980; Sorrell and Dromgoole, 1986). Differences between species in their ability to store O_2 within the lacunae of the leaves are known to exist (Sand-Jensen et al., 1982), as already discussed. Similarly, differences with

respect to exchange of CO_2 have also been demonstrated. In thin leaved species, such as *Elodea*, which possess few or no lacunae, release of respired and photorespired CO_2 from the leaf is favored. In *Lobelia* and other isoetids that are characterized by large lacunar volumes, internal O_2 storage is promoted (Søndergaard, 1979). Additional evidence also suggest that plants intermediate in these characteristics show intermediate lacunar storage capabilities (Søndergaard and Wetzel, 1980). Collectively, these results suggest that features which promote gas exchange across the leaf surface facilitate both the uptake of CO_2 and release of O_2. Those that restrict exchange across the leaf surface promote the recycling of both of these gases within the lacunar system. It is not surprising then, to note that in *Lobelia* and other species of similar growth form, much of the CO_2 fixed during photosynthesis is not taken up over the leaf surface but is taken up over the root surface and is transported to the leaves via the lacunar system (Wium-Andersen, 1971; Søndergaard and Sand-Jensen, 1979; Wetzel et al., 1985).

The purpose of this investigation was to examine the general anatomy and ultrastructure of leaves of the selected submersed species and to identify features which may influence either the release of gases across the leaf surface or their accumulation within the lacunar system. Although many studies have examined the ultrastructure of leaves of different seagrass species (Jagels, 1973; Birch, 1974; Doohan and Newcomb, 1976; Benedict and Scott, 1976; Barnabas et al., 1977; Kou, 1978; Barnabas et al., 1980; Barnabas, 1982; Cambridge and Kou, 1982), comparatively few freshwater species have been investigated (Falk and Sitte, 1963; Sitte, 1963; Lunney et al., 1975; Pendland, 1979; Valanne and Rintamaki, 1982), none of which specifically examine structural resistances to gas exchange.

RESULTS

Elodea

With the exception of the midvein region, the leaf of *Elodea* consisted entirely of two epidermal cell layers and measured 50-75 μm thick (Figure 1). Cells of the upper epidermis appeared approximately 8 times as large as those of the lower epidermis and accounted for roughly 2/3 of the total leaf thickness (Figure 1, 2). Cells were rectangular in shape and arranged in files along the length of the leaf (Figure 2). Small triangular to diamond-shaped intercellular gas spaces, measuring 10 to 20 μm across, were regularly found at the junction where the radial walls of the upper epidermal cells meet the adjacent radial walls of the lower epidermal cells (Figure 1). Due to the difference in their sizes, each cell of the upper epidermis bordered upon two of these gas spaces whereas cells of the lower epidermis normally bordered upon only one. The gas spaces also extend vertically down the leaf blade, and are thought to be continuous throughout its length (Dale, 1957a). The midvein was multi-layered, cells were densely packed and relatively devoid of gas spaces (not shown).

The outer epidermal wall was much thicker than either the inner tangential or radial walls (Figure 1, 3). On the lower epidermis, the inner half of this wall exhibited a cross-hatched lamellate texture (Figure 4), a feature commonly observed in the walls of epidermal (Chafe and Wardrop, 1972) and collencyhma cells (Chafe, 1970). In cells of the upper epidermis, the lamellate structure often appeared loose and disorganized (Figure 5). The outer half of the epidermal cell wall was homogenous in appearance and uniformly covered with a thin (30 nm) electron translucent cuticular layer (Figure 6, 7). Several cone-shaped areas or pores were commonly found in the cuticle of the lower

epidermis (Figure 7). They appeared to completely traverse this layer (Figure 8). These structures were rarely observed in the cuticle of the upper epidermis (Figure 6). The cuticle was often covered with a thin electron-dense layer to which the periphytic community is loosely associated (Figure 7).

A distinct feature of the lower epidermis was the presence of several finger-like extensions of the cell wall which project from the outer tangential wall into the cell cavity (Figure 4). The plasma membrane was highly convoluted around these extensions. Mitochondria with prominent cristae were found concentrated in this region. Cells with such wall ingrowths are termed "transfer cells" and, due to the proliferation of the plasma membrane around these extensions, possess a high surface area:volume ratio (Gunning and Pate, 1969).

The striated pattern of the epidermal wall appeared to be continuous around the entire cell, including the gas spaces (Figure 9, 10). In the corners of the gas spaces, a slight thickening of the wall was observed. At the junction where gas spaces were not produced, triangular thickenings in the wall were found (Figure 3). Plasmodesmatal connections were frequently observed between adjacent cells of the same epidermal layer (Figure 9), as well as between epidermal layers (Figure 10).

In all sections examined, chloroplasts were found distributed equally along the walls of lower epidermal cells and randomly throughout cells of the upper epidermis (Figure 1). They were not found appressed against the outer wall as is commonly observed in leaves of submersed plants (Sculthorpe, 1967). Chloroplasts were characterized by well-developed grana, numerous osmiophilic bodies and large starch grains which often distorted their shape (Figure 3, 9, 10).

Myriophyllum

The fine cylindrical leaflet of *Myriophyllum* measured less than 0.5 mm in diameter and consisted of a single layer of small epidermal cells and an undifferentiated mesophyll that surrounded a central core of vascular tissue (Figure 11). The mesophyll was 3 to 5 cells thick. Cells were round to oval in shape and tightly packed together. Occasionally small triangular to diamond shaped intercellular gas spaces, measuring 2-10 μm across, were visible in the light microscope. They appeared scattered randomly throughout the mesophyll and were not as large or abundant as those depicted in the leaflet of the related species *M. spicatum* (Hasman and Inanc, 1957; Grace and Wetzel, 1978).

The rachis showed similarities to both the leaflets and the stem (Chapter II) in general anatomy (Figure 12). The outer mesophyll consisted of a layer of 2-5 closely packed round cells. Within the inner mesophyll, cells were arranged in a fashion similar to those of the middle cortex of the stem and formed a single ring of small lacunae that encircles the vascular cylinder. These gas spaces were round to oval in shape and range from 10-40 μm in diameter. Chloroplasts were abundant and distributed equally throughout both the epidermis and mesophyll.

Epidermal cells were arranged in files along the length of the leaflet (Figure 13). They contained several chloroplasts that were commonly found lining the relatively thick outer cell wall (Figure 11, 14). The epidermis was covered by a thin (60 nm), finely reticulate cuticular layer (Figure 14, 15).

Triangular thickenings in the cell wall were observed at the point where adjacent epidermal cells met underlying mesophyll cells (Figure 14). They were also found

throughout the mesophyll at the common junction between 3 or 4 adjacent cells (Figure 16). Wherever gas spaces were produced, they were found at the center of these thickenings (Figure 17).

The mesophyll consisted of uniformly thin-walled cells that, like epidermal cells, were highly vacuolate and frequently filled with darkly staining material (Figure 11, 17). Chloroplasts were long and thin and often contained large starch grains (Figure 14, 16, 17). Plasmodesmatal connections were not observed between adjacent epidermal cells (Figure 14), but were frequently found between mesophyll cells (Figure 16).

Potamogeton

The broad leaves of *Potamogeton* show major differences between the leaf blade proper and the minor and central midvein regions (Figure 18, 19). The leaf blade measured roughly 50 μm thick and consisted of two epidermal cell layers and a single layer of intervening mesophyll cells (Figure 18). Both epidermal layers appeared identical in gross anatomy and were similar to the mesophyll in both size and shape. Small and inconspicuous gas spaces were occasionally produced at the junction of the mesophyll and epidermis. They were not, however, a regular or consistent feature in this region of the leaf. Around the minor veins, the mesophyll may become 2 or more cell layers thick. In this region a few small gas spaces were commonly found around the vascular bundles (not shown). In the thicker midvein region, however, large, round to oval shaped gas lacunae that measure 100-200 μm in diameter surrounded the vascular bundle (Figure 19). The gas spaces formed continuous canals along the length of the leaf, and were frequently traversed by diaphragms like those found in the stem (ChapterII).

The two epidermal layers appeared symmetrical (Figure 18); no major anatomical or ultrastructural differences could be identified. The outer epidermal wall was several times as thick as both the inner tangential or radial walls (Figure 20). Microfibrils which form the inner layer of the outer epidermal wall appeared swollen and loosely organized (Figure 21). It is bound by a thin (50 nm) amorphous electron translucent cuticle, which was often covered by a layer of flocculent electron dense material (Figure 21).

The internal walls were variable in thickness (Figure 22, 23). Plasmodesmata were abundant and found in the constricted areas of the walls bordering the mesophyll (Figure 22, 23).

Chloroplasts were abundant and appeared distributed evenly throughout both the epidermal and mesophyll layers. Chloroplasts of the epidermis commonly contained large stacks of grana, osmiophilic bodies and often several small starch grains (Figure 20). Starch grains in the chloroplasts of the mesophyll, however, were usually much larger (Figure 18, 20, 23). Large starch grains were also found in the mesophyll cells surrounding the veins (Figure 19). This pattern of starch distribution appears to be characteristic of the leaf of this species (Hough and Wetzel, 1977).

Lobelia

The strap-shaped leaf of *Lobelia* measured 1-5 mm in diameter and appeared in cross-sectional view like two hollow tubes of mesophyll cells that were linked together in the middle by a bridge of mesophyll tissue (Figure 24). This arrangement results in the formation of two large gas lacunae, measuring roughly 0.5 mm in diameter, that formed continuous canals along the length of the leaf. The mesophyll consisted of 4 or more layers of round to oval shaped cells (Figure 25). In addition to the large gas

lacunae, intercellular gas spaces of various shapes and sizes, ranging from 1-10 μm across, were commonly found at the junction between adjacent cells (Figure 25). These gas spaces were also likely to form continuous, although indirect, gas pathways between cells of the mesophyll and the central lacunae.

The leaves examined were encrusted with a dense periphytic community dominated by diatoms (Figure 26). The surface of the leaf underneath this layer was undulating and irregular in appearance (Figure 27), a pattern also seen in cross-sectional view (Figure 28). The relatively thick outer epidermal wall appeared uniform in texture and was covered by a thick (1.1 μm) cuticle (Figure 28). The cuticle consisted of a thin inner reticulate layer and an outer amorphous region. Members of the periphytic community were confined to the electron dense matrix that surrounds the leaf and did not appear to disrupt or penetrate the cuticle.

Cells of the epidermis consisted of a large central vacuole filled with electron dense material and a thin layer of cytoplasm in which a few organelles were found (Figure 28, 29). Mesophyll cells had uniformly thin walls and contained numerous chloroplasts (Figure 25). Chloroplasts were most abundant in cells underlying the epidermis and decreased in numbers toward the large central gas lacunae. They were round to oval in shape, and contained several osmiophilic bodies, but relatively little starch (Figure 29). Plasmodesmata were observed between adjacent epidermal cells and between epidermal and mesophyll cells, but were most frequently produced between adjacent mesophyll cells.

Occasionally, plasmolyzed cells containing senescent chloroplasts and vesiculate debris were found in the mesophyll (Figure 30). These cells were usually isolated and

bordered upon normal and unaffected cells. Vesiculate material was also found within the gas spaces adjacent to these cells.

Figure 1. Cross-section of *Elodea* leaf. Light micrograph showing size and arrangement of epidermal cell layers and the distribution of gas spaces. Bar=50 μm.

Figure 2. Surface view of *Elodea* leaf. SEM micrograph of A) upper and B) lower leaf surface. Note differences in cell sizes between cell layers. Bar=50μm.

Figure 3. Lower epidermis of *Elodea* leaf. TEM micrograph showing structure of chloroplasts and differences in wall thickness. Bar=50 μm.

Figure 4. Lower epidermis of *Elodea* leaf. Outer wall showing lamellate structure of wall and transfer cell characteristics. Arrows pointing to wall lamellations (WL). Bar=1 μm.

Figure 5. Upper epidermis of *Elodea* leaf. TEM micrograph of outer wall showing loosened and disorganized inner layer (arrows). Bar=1 μm.


1

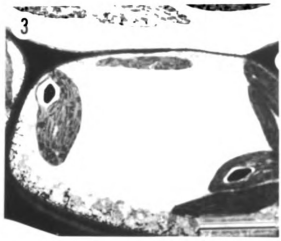
3

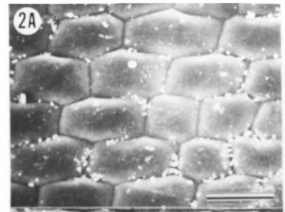
2A

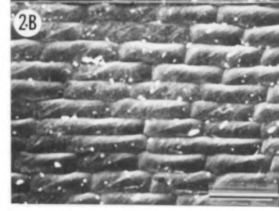
2B

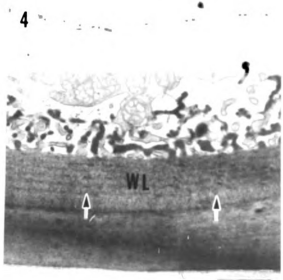
4
WL

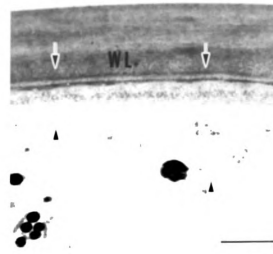
5
WL

Figure 6. Upper epidermis of *Elodea* leaf. TEM micrograph showing electron translucent cuticle (delineated by arrows). Bar=0.25 μm.

Figure 7. Lower epidermis of *Elodea* leaf. TEM micrograph of cuticle and attached members of the periphytic community. Bar=0.25 μm.

Figure 8. Lower epidermis of *Elodea* leaf. TEM micrograph of pores (P) traversing the cuticle. Bar=0.05 μm.

Figure 9. Cross-section of *Elodea* leaf. TEM micrograph illustrating gas space (GS) between cells of lower epidermis. Wall is striated in appearance, contains plasmodesmata (PD) and is thickened in the corners of the gas space. Bar=2.5 μm.

Figure 10. Cross-section of *Elodea* leaf. TEM micrograph of common cell wall between epidermal layers containing numerous plasmodesmata (PD). Chloroplasts contain large starch granules. Bar=2.5 μm.

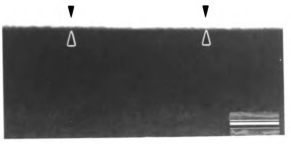
6

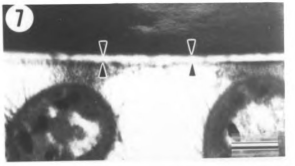
7


8
P
P

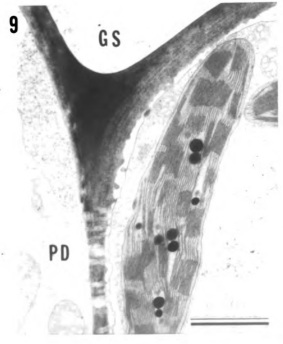
9
GS
PD

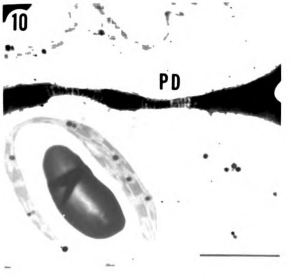
10
PD

Figure 11. Cross-section of *Myriophyllum* leaflet. Light micrograph showing size and arrangement of cells. Bar=0.05 mm.

Figure 12. Cross-section of *Myriophyllum* rachis. Light micrograph showing size and distribution of gas lacunae (marked by arrows). Bar=0.05 mm.

Figure 13. Surface of *Myriophyllum* leaflet. SEM micrograph. Bar=25 μm.

Figure 14. Epidermis of *Myriophyllum* leaflet. TEM micrograph of epidermal cell showing chloroplast structure, differences in cell wall thickness and relative thickness of cuticle. Bar=5 μm.

Figure 15. Epidermis of *Myriophyllum* leaflet. TEM micrograph of finely reticulate cuticle (delineated by arrows). Bar=0.25 μm.

Figure 16. Mesophyll of *Myriophyllum* leaflet. TEM micrograph showing junction of 3 mesophyll cells and triangular thickening of common cell wall. Bar=0.25 μm.

Figure 17. Mesophyll of *Myriophyllum* leaflet. TEM micrograph of diamond-shaped gas space (GS) produced at junction between 4 adjacent mesophyll cells. Plasmodesmata present between mesophyll cells. Bar=5 μm.


11

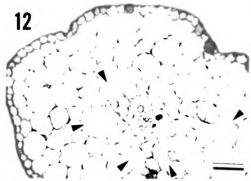
12

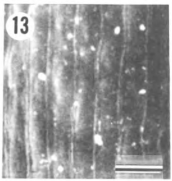
13


14

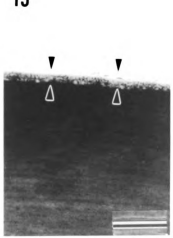
15


16

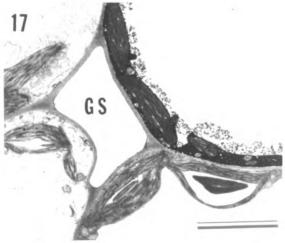
17
GS

Figure 18. Cross-section of *Potamogeton* leaf blade. Light micrograph showing size and arrangement of cells. Bar=50 μm.

Figure 19. Cross-section of *Potamogeton* leaf at midvein. Light micrograph showing size and arrangement of cells and the distribution of gas lacunae (GL). Bar=0.2 mm.

Figure 20. Epidermal cell of *Potamogeton* leaf. TEM micrograph showing relatively thick outer cell wall and chloroplasts with small starch grains. Underlying mesophyll (M) contains chloroplasts with large starch grains. Bar=5 μm.

Figure 21. Epidermal cell wall of *Potamogeton* leaf. TEM micrograph showing relative thickness of cuticle (delineated by arrows) and loosened appearance of inner wall (arrows with tails). Bar=0.05 μm.

Figure 22. Cross-section of *Potamogeton* leaf. TEM micrograph at the junction of epidermis and mesophyll, showing plasmodesmata (PD), variable wall thickness and lack of gas spaces. Bar=0.05 μm.

Figure 23. Cross-section of *Potamogeton* leaf. TEM micrograph at the junction of epidermis (EP) and mesophyll (M) showing small gas space (GS), plasmodesmata (PD) and differences in chloroplast structure. Bar=0.25 μm.

18

19

20

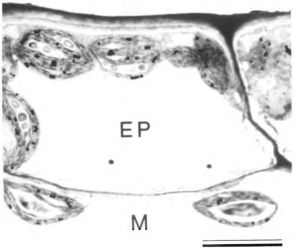

21

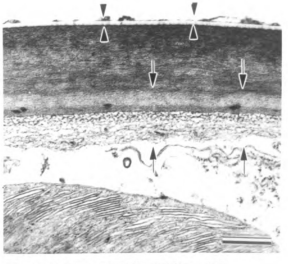

22

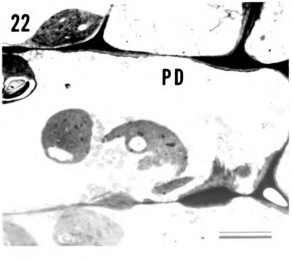

23

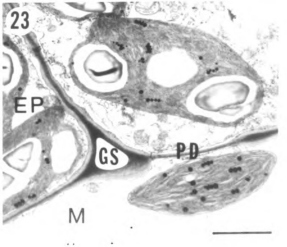

Figure 24. Cross-section of *Lobelia* leaf. Light micrograph showing large central gas lacunae (GL). Bar=0.2 mm.

Figure 25. Cross-section of *Lobelia* leaf. Light micrograph showing distribution of chloroplasts primarily in cells underlying the epidermis. Arrows pointing to intercellular gas spaces contiguous with gas lacunae (GL). Bar=50 μm.

Figure 26. Surface of *Lobelia* leaf. SEM micrograph of periphytic community present on leaf surface. Bar=0.1 mm.

Figure 27. Surface of *Lobelia* leaf. SEM micrograph of leaf surface. Bar=0.1 mm.

Figure 28. Epidermis of *Lobelia* leaf. TEM micrograph showing structure and thickness of cuticle (delineated by arrows) and composition of the periphytic community. Bar=5 μm.

Figure 29. Cross-section of *Lobelia* leaf. TEM micrograph at junction of epidermis (EP) and mesophyll (M) showing development of gas space (GS), the lack of chloroplasts in the epidermis and their abundance in underlying mesophyll cells. Bar=10 μm.

Figure 30. Mesophyll of *Lobelia* leaf. TEM micrograph showing chloroplast degradation, storage of vesiculate material (VM) in cells and gas spaces (GS), as well as healthy mesophyll cells. Bar=10 μm.

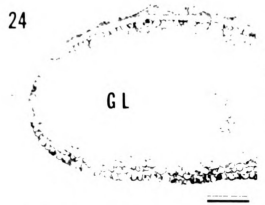
24
GL


25
GL

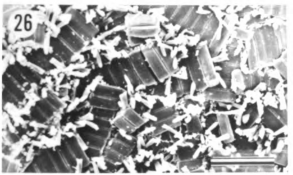
26

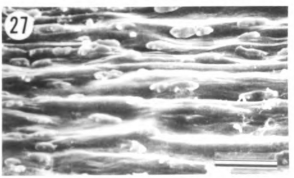
27


28


29
EP
GS
M

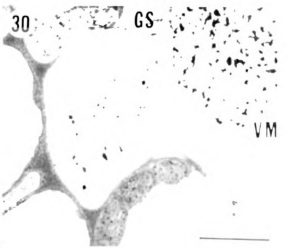
30
GS
VM

DISCUSSION

In submersed plants, O_2 produced during photosynthesis either accumulates within the lacunar atmosphere or is released to the surrounding water (Hartman and Brown, 1967). The direction of O_2 flow or the partitioning between these two phases, as described by Fick's first law, is determined by the surface area, the resistance to gas flow and the O_2 gradient (Browse et al., 1977; Payne, 1983). O_2 released from the leaf must diffuse from the chloroplast to the bulk water phase. In this path it encounters resistances associated with transport from the chloroplast to the epidermis as well as diffusion through the outer epidermal wall and the surrounding boundary layer. Accumulation of O_2 within the lacunar atmosphere, on the other hand, involves only the internal resistances of the leaf tissue to gas transport (Sorrell and Dromgoole, 1986).

Diffusion of O_2 from the chloroplast to the lacunae occurs in the aqueous phase and the resistance it encounters is directly related to the length of the diffusion pathway (Browse, et al., 1977). The internal resistance to O_2 diffusion in leaves of *Elodea* would be expected to be relatively minor since both epidermal layers bordered upon at least one gas space. Gas spaces, however, were not produced between each cell in leaves of *Potamogeton* and *Myriophyllum*. In these leaves the distance between chloroplasts and lacunae may often be several cells in length. If the resistance to lateral transport over this distance is greater than the resistance through the epidermis, release of O_2 from the leaf would be expected. In *Lobelia*, chloroplasts were found throughout the mesophyll, but were not present in the epidermis. Although the mesophyll was several layers thick, O_2 transport through this layer is likely to occur through the intercellular gas spaces that

appear to be continuous with the central lacunae. This feature would not only facilitate the transport of O_2 but also the transport of CO_2 from the central lacunae to the outer mesophyll where chloroplasts were abundant.

When the resistance to O_2 release is high or the gradient between the lacunae and the surrounding water is low, accumulation of O_2 within the lacunar system is favored. As O_2 accumulates within the lacunar atmosphere, the O_2 partial pressure increases and when the O_2 gradient overcomes the resistance to outward diffusion, release of O_2 will occur. The steepness of this gradient will be determined by the lacunar volume and pressure, the photosynthetic rate and the rate at which O_2 is removed from the leaf as it is transported down the stem and into the roots (Chapter II), (Sand-Jensen and Prahl, 1982; Sorrell and Dromgoole, 1986).

The diffusion of gases through the boundary layer provides the major resistance to CO_2 uptake in leaves of submersed plants and can limit the rate of photosynthesis, even under well-stirred conditions (Browse et al., 1979; Smith and Walker, 1980; Black et al., 1981). Since O_2 diffuses along the same pathway (Armstrong, 1979), it is also likely to provide a significant resistance to O_2 release. The increase in the rate of O_2 release observed with increasing current velocities, and hence decreasing boundary layer thickness, supports this conclusion (Westlake, 1967; Madsen and Søndergaard, 1983; Sorrell and Dromgoole, 1987).

The cuticle of submersed vascular plants is typically very thin and is thought to provide little or no resistance to the diffusion of gases or solutes (Sculthorpe, 1967; Sharpe and Denny, 1976; Denny, 1980). Although the resistance of the cuticle of submersed plants to the diffusion of gases has not been examined directly, the cuticle of

Potamogeton lucens was found to provide some resistance to the diffusion of water, although 1,000 times less than that of terrestrial species (Schönherr, 1976).

The electron translucent cuticles of *Elodea*, *Myriophyllum*, and *Potamogeton* appeared to ultrastructurally similar to cuticles of other freshwater submersed plant species (Sharpe and Denny, 1976; Halloway, 1982). They were all of similar thicknesses (0.03-0.06 μm). The thick (1.1 μm) cuticle of *Lobelia*, on the other hand, resembles the cuticle of many terrestrial species, both in size and structure (Halloway, 1982). If similar resistances can also be expected, the cuticle should offer a substantial resistance to gas exchange since the cuticle of terrestrial plants provides an effective barrier which minimizes passive water loss across the leaf (Ting, 1982).

The lower epidermis of *Elodea* was associated with the presence of several small, electron dense areas or pores which traverse the cuticle. Structures of this nature have not been reported elsewhere for submersed plants.

The periphytic community was embedded in a matrix of electron dense material that did not appear to attach directly to the cuticle. Cellulolytic bacteria have been isolated from members of this community (Robb et al., 1979) and may be associated with cuticular peeling and rupture of the epidermal cell wall (Howard-Williams, et al., 1978). Bacterial colonization of the leaf surface has also been correlated with a progressive internal disorganization of the epidermis, a swelling and loosening of the cell wall, followed by invasion into the epidermis and mesophyll and ultimately cell death (Rogers and Breen, 1981). The inner portion of the outer epidermal wall appears swollen and loosely organized in leaves of both *Elodea* and *Potamogeton*, and may be undergoing the initial stages of senescence as characterized above (Rogers and Breen, 1981). In none

of the leaves examined by TEM was there evidence of direct bacterial damage to the cuticle or epidermis. Unfortunately surfaces of these leaves were not viewed by SEM at magnifications necessary to examine the extent of this activity. Rogers and Breen (1981), however, note that swelling and disorganization of the epidermal wall can result without extensive damage to the leaf surface.

The effects of these bacteria on the leaf surface can be seen within 6 weeks after emergence and within 14 weeks can result in leaf senescence (Howard-Williams et al., 1978). In *Elodea*, *Potamogeton* and *Myriophyllum*, where growth rates are relatively high, a significant proportion of the leaf biomass may die before the seasonal maximum is attained (Rich et al., 1971; Adams and McCraken, 1974). The evergreen leaves of *Lobelia* examined in this study may be close to one year old (Moeller, 1978). The degradation of chloroplasts and the storage of vesiculate material within a few cells of the mesophyll may be interpreted as symptoms of an age related process (Mahlberg, 1972). It is therefore surprising that the well-developed periphytic community present on the leaves of *Lobelia* had no apparent effects of the cuticle surface or on the ultrastructure of the epidermis. In this slow growing annual, the thick cuticle may provide a substantial resistance not only to gas exchange, but also to the pathogenic effects of the periphytic community.

CHAPTER II

ANATOMY OF THE LACUNAR SYSTEM: STRUCTURAL RESISTANCES TO GAS TRANSPORT

INTRODUCTION

Although gas spaces are found throughout the plant kingdom, they reach their greatest development, in terms of both size and proportion, within tissues of aquatic plants (Sifton, 1945; 1957).

Gas spaces develop by either schizogeny or lysigeny. Schizogenous gas spaces arise by the splitting apart of the common wall between adjacent cells and include the small intercellular gas spaces as well as the large gas lacunae characteristically found in leaves and stems of submersed plants. In *Elodea*, stem lacunae are initiated at the shoot apex as small intercellular spaces and attain their characteristic size and shape by the regular growth and development of bordering cortical cells (Dale, 1957a). These lacunar initials are thought to form due to increasing O_2 pressures which develop in the stem during photosynthesis (Dale, 1957b). Lysigenous gas spaces result from cell death and disintegration. They are common not only in roots of aquatic plants, but also develop in the roots of many terrestrial species that are able to survive waterlogging conditions (Sifton, 1945; 1957; Kawase, 1981).

It is commonly stated that the lacunar system of submersed macrophytes occupies a significant, yet variable, proportion of the total plant body and that it serves as both a reservoir for the storage of O_2 and as a pathway for its transport (Sculthorpe, 1967; Hutchinson, 1975; Wetzel, 1975). Little, however, is actually known about the variation that exists between species and the functional significance of these differences with respect to gas transport.

A number of recent studies have established a correlation between the ability of submersed plants to transport and release O_2 from their roots and the degree of their lacunar development . As already discussed, the results of Sand-Jensen et al. (1982) show that the isoetid species, with their large lacunar volumes, are better adapted to O_2 transport than species characterized by small lacunar volumes. Penhale and Wetzel (1983) noted an increase in the lacunar development of roots of seagrasses distributed along a gradient of increasing sediment O_2 demand and suggested that plants with the more developed lacunar system would facilitate higher O_2 flux rates. Smith et al. (1984) observed higher rates of O_2 release from roots of mature seagrasses; young individuals were characterized by poorly developed lacunar systems. In *Potamogeton perfoliatus*, Kemp and Murray (1986) found that the amount of O_2 released from the roots was inversely related to the overall length and mass (specific gravity) per unit length of the stem. Their results suggest that both a decrease in the length of the pathway and an increase in percentage gas space or porosity, as reflected by low mass per unit stem length, increases the rate of transport from the shoots to the roots.

Armstrong (1979) examined the inter-relationship of porosity and path length on the transport of O_2 down the roots by measuring its release from the roots. Increases in

porosity were found to have more of an overall effect on reducing resistance than decreases in root length. This is due, at least in part, to proportionate decreases in the amount of respiring tissue (Williams and Barber, 1961; Armstrong, 1972; 1979; Penhale and Wetzel, 1983). Length of stems and roots are known to vary with both age and environmental conditions (Sculthorpe, 1967). Lacunae, on the other hand, can form relatively consistent patterns within tissues of submersed plants (Arber, 1920; Sculthorpe, 1967). Porosity should therefore be a reliable feature on which to evaluate the efficiency of lacunar transport, provided that no additional barriers to transport exist.

The purpose of this investigation was twofold. First, to examine the anatomy and continuity of gas spaces throughout the plant body and to identify features which may restrict or impede gas transport. And secondly, to evaluate the functional significance of the lacunar system in gas transport by examining differences in porosity that may exist between the selected species.

RESULTS

Elodea

The gas space system of the mature *Elodea* stem was characterized by a double ring of large gas lacunae that encircled the stem throughout the middle cortex (Figure 31). The lacunae were round to oval in shape and were formed by the arrangement of cells into single rows or files which interconnect in honeycomb pattern. The lacunae also extended vertically down the stem to form gas canals that were continuous throughout the length of the internode (Figure 32). In the stems examined, the lacunae ranged from 25-200 μm in diameter and occupied over 30% of the cross-sectional area of the cortex or roughly 26% of the volume of the internode (Table 1).

Throughout the inner and outer cortical regions, small intercellular gas spaces, measuring 1 or 2 μm in diameter, were also produced (Figure 31). They were not common, however, at the junction between epidermal and underlying cortical cells. The vascular tissues were densely packed and also devoid of obvious gas spaces.

The lacunar system of the mature sediment roots of *Elodea* examined consisted entirely of small intercellular gas spaces of schizogenous origin (Figure 33). Gas spaces were found throughout the cortex and were regularly produced at the junction between 4 or more adjacent cells. They ranged from 4- to 10-sided polygons in shape and varied from 10-50 μm in diameter. Gas spaces occupied approximately 33% of the cortical area or roughly 22% of the volume of the root (Table 2, 3).

The root was bound by a single layer of large epidermal cells (Figure 33). (Chapter III). Gas spaces were not common at this junction nor were they prominent between cells of the vascular cylinder.

Vascular traces to both the leaves and the roots cross the cortex of the stem at the nodes (Dale, 1957a) (not shown). In regions unoccupied by these tissues, small plates of cells, called diaphragms, were found traversing the large gas canals (Figure 34, 35). Diaphragms were usually 1, sometimes 2 cell layers thick and were made up of hexagonally shaped cells (Figure 36). Small triangular gas spaces or pores, measuring roughly 2-5 μm across, were present at the corners where 3 adjacent cells of the diaphragm met. The effect of diaphragms on gas transport is examined in Chapter IV.

Leaves were inserted into the node through a slight constriction at their bases. The smaller cells of the lower epidermis enlarge at this junction (not shown) and although this enlargement should also result in the formation of larger gas spaces, their continuity with the stem could not be verified. The junction of the mature root to the stem was not examined.

Myriophyllum

The most striking feature of the stem of *Myriophyllum* was the highly lacunate structure of the middle cortex (Figure 37). Cells in this region were rectangular in shape and arranged end-to-end in single file. Columns of these cells bridge the outer and inner cortical regions and radiate around the stem much like the spokes of a wheel. A single oval-shaped lacuna was formed between the columns. The lacunae also extended longitudinally down the stem and formed gas canals that were continuous throughout the length of the internode. In the stems examined, the lacunae measured roughly 100 μm wide and 400 μm long and accounted for more than 50% of the area of the cortex or roughly 48% of the stem's volume (Table 1, 3).

Between cells of the inner and outer cortex, small intercellular gas spaces, measuring 1-2 μm in diameter were produced (not shown). The cortex was tightly bound by a single layer of small epidermal cells (Figure 37). Gas spaces were absent at this junction and within tissues of the central vascular cylinder.

Both lysigenous and schizogenous gas spaces were produced in the mature root of *Myriophyllum* (Figure 38). Lysigenous gas spaces extended primarily from the outer to the mid-cortical region and were formed by the collapse of radially aligned groups of cells. The walls of these cells produced thin partitions which separate adjacent lacunae. Small diamond-shaped schizogenous gas spaces were found between the apparently healthy cells that scattered throughout the cortex. Collectively, these gas spaces occupied around 46% of the cortical area or roughly 32% of the volume of the roots examined (Table 2, 3).

The outermost protective layer of the root consisted of 3 or more layers of densely packed, thick walled cells that were irregular in shape (Figure 38) (Chapter III). Gas spaces were not found between cells of this layer. They were also absent within the tissues of the vascular cylinder.

Leaves are usually arranged in whorls about the node and are directly inserted into the stem by the rachis. The lacunae of the rachis appeared uninterrupted up to their insertion into the stem (Figure 39). It could not be determined whether the gas spaces of the rachis formed a continuous pathway through these layers to the lacunae of the stem.

The gas canals of the stem, although continuous throughout the length of the internode, were interrupted at the node by diaphragms and tissues associated with leaf

traces (Figure 39, 40). The leaf trace consisted of a core of vascular tissue surrounded by a compact layer of parenchyma cells embedded within a multi-layered sheath of small globose cells (Figure 41). Intercellular gas spaces, roughly 10 μm across, were present at the rounded corners of these cells. The influence of diaphragms on gas transport is examined in Chapter IV.

Rhizomes were similar to the stem in general anatomy (Figure 39, 42). The vascular traces to the numerous adventitious roots could be seen traversing the cortex of the rhizome (Figure 42). The gas spaces of the root appeared to be continuous from the external root into the tissues of the root trace. The root trace, like the leaf trace, was also surrounded by several layers of small globose parenchyma cells. The pathway across this tissue could not be determined.

Potamogeton

In the stems on *Potamogeton*, cells of the cortex were arranged into single rows or files of cells which interconnect at right angles and form a honeycomb or net-like pattern (Figure 43). This arrangement resulted in the formation of 3-5 rings of large, round to oval-shaped gas lacunae that encircle the stem. The lacunae typically ranged from 50-350 μm in diameter and decreased in size toward the center of the stem. They occupied nearly 70% of the cortical area or roughly 63% of the volume of the internodes examined (Table 1, 3).

At the outer edge, the stem was bound by a layer of small square-shaped epidermal cells and a single layer of underlying cortical cells (Figure 44). Gas spaces were not abundant at this junction. The vascular cylinder was surrounded by layer of 3 to 5 cortical cells (Figure 45). Small intercellular gas spaces, measuring 1-2 μm in

diameter, were produced between these cells. Gas spaces were not obvious between cells of the vascular tissues.

The mature root of *Potamogeton* contained both lysigenous and schizogenous gas spaces (Figure 46). Collectively, these gas spaces accounted for 61% of the total cross-sectional area of the cortex or roughly 46% of the volume of the roots examined (Table 2, 3). Lysigenous gas spaces developed only in the outer third of the cortex and formed a concentric ring around the root. The gas spaces appeared to be continuous along the length of the root, but were separated radially by thin partitions formed by remains of collapsed cell walls. Cells of the middle and inner cortex appeared round, turgid and apparently in healthy condition. Small diamond-shaped, schizogenous gas spaces, measuring roughly 10 μm across, were formed between these cells.

The cortex was bound at the outer edge by a single layer of large, turgid cortical cells and a layer of small thick walled, irregularly shaped hypodermal cells (Figure 46). Gas spaces were not found between cells of these two layers (Chapter III) nor are they present between tissues of the vascular cylinder.

The gas canals of the stem were frequently interrupted throughout the length of the internode (Figure 47) as well as at the node (Figure 48) by the presence of horizontal diaphragm plates. Diaphragms consisted of a single layer of small, hexagonally shaped cells which produced small triangular pores at their corners (Figure 49). The effect of these diaphragms on gas transport is examined in Chapter IV.

The leaf attaches to the stem through a constriction at its base. At this junction, the gas spaces surrounding the veins of the leaf (Chapter II) enlarge considerably and

appear to merge into the tissues of the stem (Figure 50, 51). It could not be determined if these gas spaces are directly continuous with those of the stem.

Rhizomes were similar to stems in general anatomy (Figure 52, 53). The gas canals of the rhizome were also traversed by diaphragms as well as by vascular traces to the many roots produced at the node. The gas lacunae of the root can be seen entering the cortex of the rhizome within the tissues of the root trace (Figure 52, 53). The traces were, however, surrounded by a few layers of small compact cells. It could not be determined whether the gas spaces of the root were continuous with the gas canals of the rhizome across this layer.

Lobelia

The stem of *Lobelia* consisted of a discrete ring of vascular tissues, a few cell layers thick, which delineated an inner pith and outer cortical region (Figure 54). Small intercellular gas spaces were interspersed throughout the large cells of the pith as well as the small globose parenchyma of the cortex. In neither of these tissues, however, were cells organized into the highly lacunate structure found in the stems of the other species examined.

The stem was not differentiated into nodes and internodes. Vascular traces to both the leaves and the roots were commonly seen traversing the outer cortical layer (Figure 55, 56). Leaves attached directly to the stem and were associated with 2 or 4 roots that were also inserted into the stem on each side of the leaf. The lacunae of both the leaves and the roots extended well into the cortical tissues of the stem (Figure 55, 56). Although it was not evident from a single cross-section, examination of a series of

sections show that the lacunar system of the leaf is continuous with the lacunae of the roots (Figure 54-56).

The cortex of the mature *Lobelia* root was occupied almost entirely by very large and irregularly shaped lysigenous gas lacunae (Figure 57). The wall remains of collapsed cortical cells formed thin partitions that traversed the cortex and, in many instances, provided the only structural connection between the inner and outer cortical regions. Small schizogenous gas spaces were also found between the remaining inner cortical cells that surrounded the vascular bundle. Approximately 75% of the cortex or roughly 58% of the root's volume was occupied by gas space (Table 2, 3).

The lacunae were bound at the epidermis by a single layer of large irregularly shaped cortical cells and a layer of small thick walled hypodermal cells (Figure 57) (Chapter III). Gas spaces were not produced between the cells of these different layers nor between cells of the vascular tissues.

Figure 31. Cross-section of *Elodea* stem. Light micrograph showing size and arrangement of gas lacunae (GL). Bar=0.2 mm.

Figure 32. Cross-section of *Elodea* stem. SEM micrograph illustrating continuity of gas canals along length of internode. Bar=0.2 mm.

Figure 33. Cross-section of *Elodea* root. Light micrograph showing size and distribution of schizogenous gas spaces (arrows). Bar=70 μm.

Figure 34. Longitudinal section of *Elodea* stem. SEM micrograph through node showing vertical distribution of gas canals and presence of diaphragms. Bar=0.2 mm.

Figure 35. Cross-section through node of *Elodea* stem. SEM micrograph showing placement of diaphragms throughout cortex. Bar=0.4 mm.

Figure 36. Cross-section through node of *Elodea* stem. SEM micrograph of diaphragm showing size and distribution of small triangular pores. Bar=50 μm.

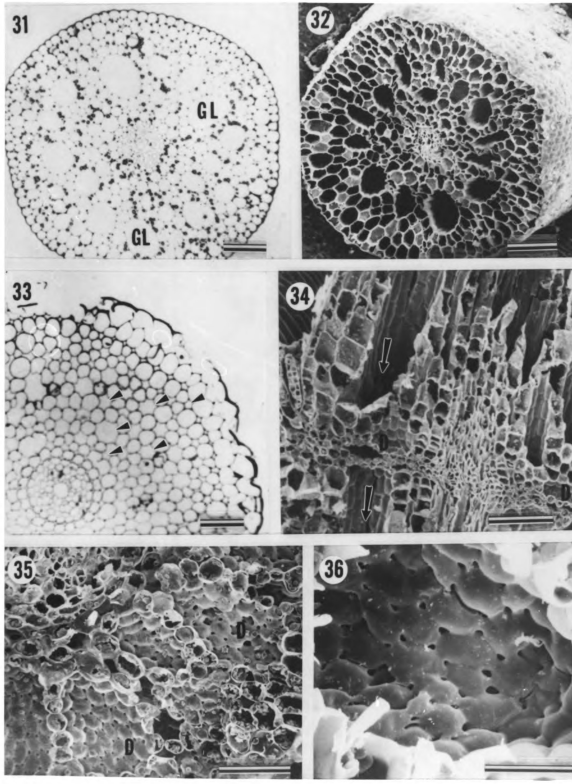
31
GL
GL
32
33
34
35
O
O
36

Table 1. Anatomical data for stems of *Elodea*, *Myriophyllum* and *Potamogeton*. Porosity expressed as mean ± standard error. * denotes significant difference ($P < 0.05$) between species. n = number of measurements.

Species	Stem Diameter (cm)	% of Total cross-sectional area			Porosity (% gas space)		
		Epidermal	Cortical	Vascular	Stem	Cortex	
Elodea	.11	15	82	3	26(±2)*	31(±2)	n=3
Myriophyllum	.15	4	93	3	48(±3)*	52(±3)	n=4
Potamogeton	.27	4	92	4	63(±3)*	69(±3)	n=3

Table 2. Anatomical data for roots of *Elodea*, *Myriophyllum*, *Potamogeton* and *Lobelia*. Porosity expressed as mean ± standard error. * denotes significant difference ($P<0.05$) between species. n = number of measurements.

Species	Root Diameter (cm)	% of Total cross-sectional area			Porosity (% gas space)		
		Epidermal	Cortical	Vascular	Stem	Cortex	
Elodea	.06	29	68	3	22(±1)*	33(±1)	n=3
Myriophyllum	.04	29	69	2	32(±4)*	46(±5)	n=4
Potamogeton	.04	21	76	3	46(±1)*	61(±1)	n=3
Lobelia	.06	22	77	1	58(±6)*	75(±6)	n=4

Table 3. Porosity values for stems and roots and relative root production of species examined.

Species	Porosity (% gas space) Stem	Root	Roots (% biomass)	Reference
Elodea	26	22	3	Borutskii, 1950.
Myriophyllum	48	32	10	Nicholson and Best, 1974. Chambers and Kalff, 1985.
Potamogeton	63	46	12 40-50	Nicholson and Best, 1974. Ozimek et al., 1974.
Lobelia	--	58	50-65	Sand-Jensen and Søndergaard, 1979.

Figure 37. Cross-section of *Myriophyllum* stem. Light micrograph showing size and arrangement of gas lacunae. Bar=0.5 mm.

Figure 38. Cross-section of *Myriophyllum* root. Light micrograph showing development of lysigenous gas spaces (GS). Bar=0.1 mm.

Figure 39. Cross-section through node of *Myriophyllum* stem. SEM micrograph showing leaf trace and part of associated sheath. Arrows denote gas pathway from leaf into stem. Bar=0.5 mm.

Figure 40. Longitudinal section through node of *Myriophyllum* stem. SEM micrograph showing insertion of diaphragm through gas canals (arrows). Bar=0.5 mm.

Figure 41. Cross-section through node of *Myriophyllum* stem. SEM micrograph of diaphragm showing size and distribution of pores (arrows). Bar=0.5 mm.

Figure 42. Cross-section through *Myriophyllum* rhizome at the junction of a root. SEM micrograph showing gas spaces of root extending into cortex. Arrows denote gas pathway from rhizome to root. Bar=0.5 mm.

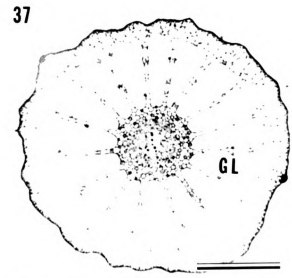
37
GL

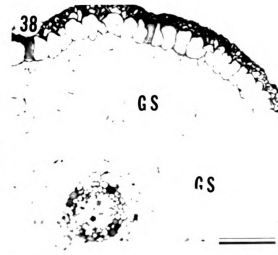
38
GS
GS

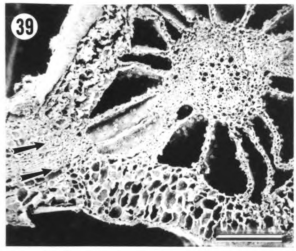
39

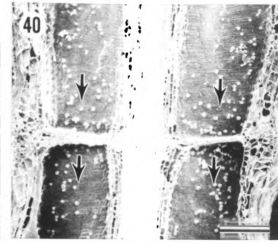
40

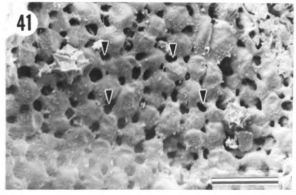
41

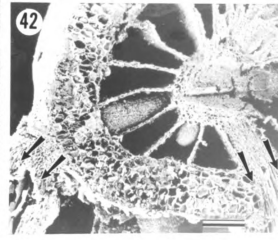
42

Figure 43. Cross-section of *Potamogeton* stem. Light micrograph showing size and arrangement of gas lacunae (GL). Bar=0.5 mm.

Figure 44. Cross-section of *Potamogeton* stem. Light micrograph of epidermis. Bar=50 μm.

Figure 45. Cross-section of *Potamogeton* stem. Light micrograph of vascular tissue. Note lack of obvious gas spaces. Bar=50 μm.

Figure 46. Cross-section of *Potamogeton* root. Light micrograph showing development of lysigenous gas spaces (GS) in outer cortex only. Bar=0.1 mm.

Figure 47. Cross-section of *Potamogeton* stem. SEM micrograph showing gas canals interrupted by diaphragms. Bar=0.1 mm.

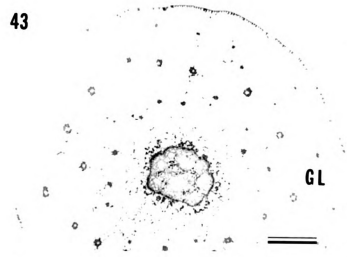
43
GL

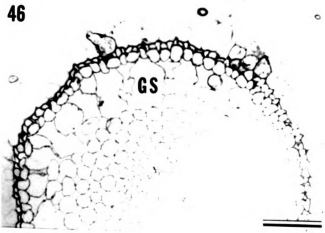
46
GS


44

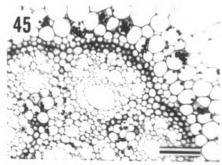
45

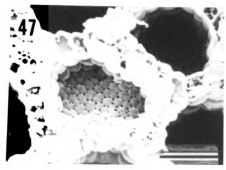
47

Figure 48. Cross-section through node of *Potamogeton* stem. SEM micrograph showing presence of diaphragms in gas canals. Bar=0.25 mm.

Figure 49. Cross-section through node of *Potamogeton* stem. SEM micrograph showing size and distribution of pores. Bar=50 μm.

Figure 50. Cross-section of *Potamogeton* stem. Light micrograph of junction of leaf. Arrows denote gas pathway from leaf to stem. Bar=0.25 mm.

Figure 51. Cross-section of *Potamogeton* stem. SEM micrograph of leaf/stem junction. Arrows denote gas pathway from leaf to stem. Bar=0.25 mm.

Figure 52. Cross-section of *Potamogeton* rhizome. Light micrograph through node showing root traces. Arrows denote gas pathway from rhizome to root. Bar=0.5 mm.

Figure 53. Cross-section of *Potamogeton* rhizome. SEM micrograph through node. Gas spaces of root appear to enter rhizome. Arrows denote pathway from rhizome to root. Bar=0.25 mm.

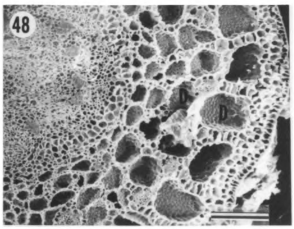
48

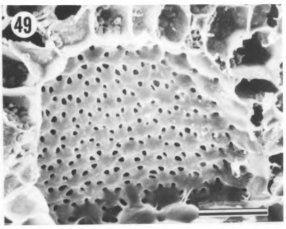
49

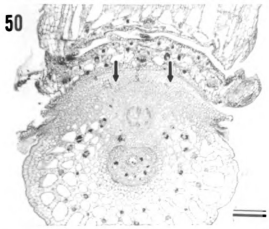
50

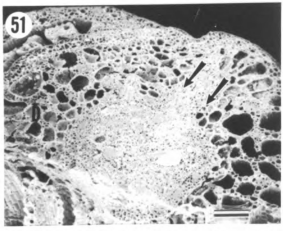
51

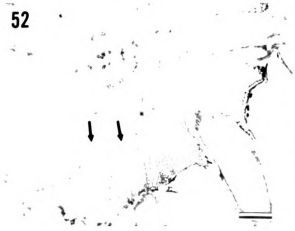
52

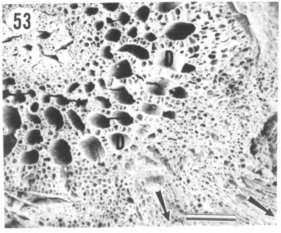
53

Figure 54. Cross-section of *Lobelia* stem. Light micrograph showing insertion of leaf. Arrows denote two large leaf lacunae. Bar=0.5 mm.

Figure 55. Cross-section of *Lobelia* stem. Light micrograph showing the close proximity of leaf and root at their insertion into the stem. Arrows denote gas pathway from leaf (2 arrows) through stem to root (1 arrow). Bar=0.5 mm.

Figure 56. Cross-section of *Lobelia* stem. Light micrograph showing insertion of leaf (1 arrow) and root (2 arrows) into stem. Bar=0.5 mm.

Figure 57. Cross-section of *Lobelia* root. Light micrograph showing lysigenous gas spaces (GS). Bar=0.1 mm.

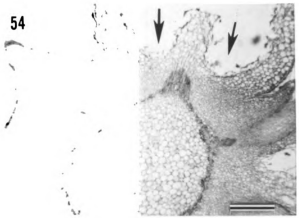
54

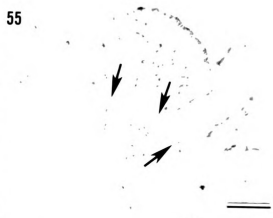
55


56

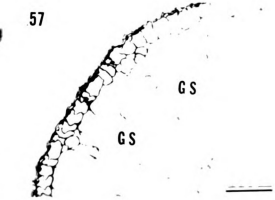
57
GS
GS

DISCUSSION

In the rosette growth form of *Lobelia*, leaves and roots are produced close together on a short compact stem. O_2 that is stored within the lacunae of the leaves (Chapter I) can be transported to the roots via an uninterrupted continuation of the lacunae throughout the stem. The short distance between leaves and roots as well as the large, continuous and uninterrupted pathway should facilitate the transport of both O_2 (Sand-Jensen et al., 1982; Sand-Jensen and Prahl, 1982) and CO_2 (Wium-Andersen, 1971, Boston et al., 1987) throughout the plant body. The segmented stems of *Elodea*, *Myriophyllum* and *Potamogeton*, on the other hand, are long and flexuous, producing leaves and roots at the nodes. This design increases not only the transport distance but also the complexity of the transport pathway. In these species, O_2 must be transported down the leaf into the stem lacunae, down the stem across several nodes to the rhizome and from the rhizome into and down the root.

The most efficient transport pathway from the leaves into the stem would be by a direct continuation between the leaf lacunae and the stem lacunae. In *Potamogeton* and *Myriophyllum*, the large gas canals surrounding the major veins of the leaf merge directly into tissues of the stem and appear to be continuous with tissues of the leaf trace. It is not clear, however, whether the gas spaces within the leaf trace are continuous with the stem lacunae. In *Elodea*, the pathway from the small gas spaces of the leaf into the stem could not be determined. If gas spaces are not continuous across this junction, O_2 transport would have to occur in an aqueous phase and the resistance associated with transport into the stem would be directly related to the length of the pathway (Sorrell and Dromgoole, 1986).

O_2 transport down the stem is facilitated by the formation of large gas canals that are continuous throughout the length of the internode. They are interrupted at the node, however, by tissues associated with traces to the leaves and roots as well as by perforated plates of cells called diaphragms. Porous diaphragms were found traversing the gas canals at the nodes of stems of *Elodea* and *Myriophyllum* and, in *Potamogeton*, were also found throughout the internode of the stem as well. The influence of diaphragms on gas transport is examined in Chapter IV. Vascular traces to the leaves and roots also traversed the stem cortex. It was not determined, however, whether these tissues completely interrupted the continuity of the intervening gas canals. If the resistance across these tissues were sufficiently high, lateral transport into adjacent gas canals might be expected. The walls bordering the lacunae were usually one cell thick and did not appear to contain pores. If lateral transport through the stem were necessary, it would likely be via aqueous diffusion through the common cell between adjacent lacunae.

In *Potamogeton* and *Myriophyllum*, the gas canals of the stem appeared to be continuous with those of the rhizome. Plants of *Elodea* do not produce a rhizome, roots arise adventitiously from the nodes of the stem. This junction was not examined. In *Myriophyllum* and *Potamogeton*, however, the root/rhizome junction is analogous to the leaf/stem junction. The gas spaces of the root appeared to be continuous within the root trace, but were bound by a few layers of cells which may provide some resistance to O_2 transport into the root. Coult (1964) described the gas pathway across the root/rhizome junction of the emergent species, *Menyanthes*, as discontinuous and, since gas spaces in this plant are as abundant within the vascular tissues as they are in the cortex, suggested that much of the O_2 transported into the root is supplied via the vascular tissues. It is

unlikely that this pathway is of any significance to O_2 transport in the species examined, since the vascular tissues of both the stems and roots are relatively devoid of gas spaces. In other emergent species, O_2 transport is thought to be continuous across the shoot/rhizome junction, although the pathway may be constricted and transport through these tissues may occur at reduced rates (Armstrong, 1979; Justin and Armstrong, 1983).

The lacunar system of *Lobelia* is continuous and provides a short and uninterrupted pathway for gas transport (Sand-Jensen and Prahl, 1982). The lacunar system has also been examined in the seagrass, *Halophila* (Roberts et al., 1984) and in *Egeria densa* (Sorrell and Dromgoole, 1986), and is thought to form a continuous pathway for transport form the shoots to the roots, In the stems of *Elodea*, *Myriophyllum* and *Potamogeton* examined in this study, the lacunar system also appeared to form a continuous pathway for O_2 transport. If the transport pathway from the leaves to the roots is not continuous in these species, and if aqueous diffusion is imposed, it is likely to occur at the junction of these organs to the stem.

In the stems of *Elodea*, *Myriophyllum* and *Potamogeton*, the lacunae varied widely in size, shape, numbers and distribution. Porosity values also differed significantly between these species and increased from *Elodea* (26%), *Myriophyllum* (48%) to *Potamogeton* (63%). The development and distribution of gas spaces in the roots also varied widely. In the roots of *Elodea*, lysigenous gas spaces were not produced. In *Potamogeton*, lysigenous gas spaces were confined to the outer cortical region, while in *Myriophyllum* and *Lobelia*, the lacunae traversed the entire cortex. Porosity values differed significantly between species and increased from *Elodea* (22%), *Myriophyllum* (32%), *Potamogeton* (46%) to *Lobelia* (58%).

Increasing porosity is known to decrease resistance and increase O_2 transport (Armstrong, 1979; Kemp and Murray, 1986). The increasing porosity of stems and roots observed in this study suggests that the ability to transport O_2 to the roots should also be expected to increase from *Elodea*, *Myriophyllum*, *Potamogeton* to *Lobelia* (Chapter IV). The amount of roots these species produce also increases respectively. These results suggest that the ability to transport O_2 to the roots is directly correlated with the amount of roots a species typically produces. In emergent plants, the ability to transport and release O_2 from the roots appears to be directly related to their distribution by determining the O_2 demand of the sediments which it can tolerate (Armstrong, 1964, 1979, Yamaski, 1987). This relationship, however, does not appear to apply to submersed plants, since *Lobelia* and related species of isoetid growth form are best able to transport and release O_2 from their roots (Sand-Jensen et al., 1982; Sand-Jensen and Prahl, 1982), yet are characteristically found in sandy sediments with low O_2 demands (Moyle, 1945; Seddon, 1972). This would suggest that submersed plants distributed in sediments with higher O_2 demands are characterized by features which decrease the amount of O_2 released from the roots. Increasing the O_2 demand of the sediments increases the O_2 gradient between the lacunar system and the water surrounding the roots. According to Fick's first law, decreasing the amount of O_2 released from the roots under conditions of increasing O_2 demand, could only occur by either decreasing the relative surface area of the roots or by increasing the resistance to diffusion across the roots (Chapter III). Decreasing the surface area across the roots can be achieved by simply decreasing the amount of roots produced. This would suggest that the distribution of submersed plants in sediments with increasing O_2 demands may be inversely related to

the amount of roots produced and, according to the results presented, a decreasing ability to transport O_2 to the roots.

CHAPTER III

ROOT ANATOMY: STRUCTURAL RESISTANCES TO GAS EXCHANGE

INTRODUCTION

Roots of submersed vascular plants are, in comparison with most terrestrial and emergent aquatic plant species, reduced both in size and structure (Arber, 1920; Sculthorpe, 1967). Although these features were at one time also interpreted as a reduction in function, a considerable amount of evidence now indicates that the roots of submersed vascular plants play a significant role in nutrient uptake (Denny, 1972; Bristow, 1975; Barko and Smart, 1981).

Aquatic sediments are often completely anaerobic a few millimeters below the sediment-water interface. The lack of O_2, however, is only one potential problem for plants rooted in these sediments. Anaerobic processes of microbes in sediments can result in the production of reduced soluble ions and volatile fatty acids which are potentially toxic to plants (Ponnamperuma, 1984; Drew and Lynch, 1980). Although some plants are temporarily able to metabolically adapt to anoxic conditions (Crawford, 1978), most aquatic plants try to avoid anoxia by transporting O_2 to the roots. O_2 transport is necessary not only to support aerobic respiratory processes but can also be utilized in the oxidation and detoxification of reduced compounds within the sediments (Armstrong, 1979, 1982; Drew and Lynch, 1981). O_2 released across the root surface

can form a protective oxidized layer immediately surrounding the root. This layer can be visualized when the rust-colored precipitates of ferric hydroxides which form upon oxidation of ferrous iron, are deposited on or around the roots (Bartlett, 1961; Green and Etherington, 1977; Chen et al., 1980; Armstrong, 1982; Taylor et al., 1984). The dimensions of this layer, and hence it oxidative ability to protect the root, will depend largely on the redox potential of the surrounding sediment and the amount of O_2 released from the root.

O_2 release from the root follows Fick's first law and is therefore a function of the surface area of the root and the resistance of the root wall to radial diffusion. The concentration difference across the root surface provides the driving force for O_2 diffusion and will determine the amount of O_2 released by a given root. In emergent species, the release of O_2 is not uniform along the length of the root but has been found to occur primarily across the root tip (Armstrong, 1964; Armstrong and Armstrong, 1988). A decrease in the sensitivity of roots of wetland plants to soil anoxia and phytotoxins has been observed upon suberization of the root wall (Sanderson and Armstrong, 1978). Suberin deposits in the wall of hypodermal cells are known to decrease the permeability of the root to both water and ions (Ferguson and Clarkson, 1976; Robards et al., 1979) and may also influence the diffusion of gases across its surface (Armstrong and Armstrong, 1988). The purpose of this investigation was to examine the general anatomy of the outer wall of roots of the selected species and to identify features which may influence the release of O_2 across this layer. Although the general anatomy of roots of several submersed species has been examined (Arber, 1920;

Sculthorpe, 1967; Tomlinson, 1969), little information exists concerning the characteristics of the outer layers of the root.

RESULTS

Elodea

Roots of *Elodea* were bound by a single layer of large epidermal cells that often appeared irregular in outline (Figure 58). These cells were highly vacuolate, contained few recognizable organelles and possessed relatively thick outer cell walls. In surface view, this wall showed evidence of epidermal pitting and peeling, presumably due to the activities of the numerous bacteria present (Figure 59). At higher magnifications, the extent of bacterial degradation became more evident. It was particularly advanced within the outer layer of this wall (Figure 60, 61) where the remaining wall material appeared as a matrix of loose fibrils of varying electron density (Figure 60). Within the inner portion of the wall electron translucent lamellae were often found in a loose transverse arrangement (Figure 60). These lamellae were similar in structure to suberin deposits found in the walls of hypodermal cells (Peterson et al., 1978). Suberin deposits, however, are not commonly observed in epidermal cells (Peterson et al., 1978).

Bacteria were not confined to the surface, but were also found throughout the wall of the epidermis. They were particularly common along the inner tangential wall between adjacent epidermal cells where the more advance stages of wall degradation usually occurred (Figure 61). The epidermis was covered by a thin, rather persistent cuticular layer which appeared to be resistant to bacterial decay (Figure 60, 61).

A layer of closely appressed cortical cells lined the epidermis (Figure 58). Gas spaces were not produced at this junction (Figure 62). A few electron-translucent lamellate structures similar to those found in the outer epidermal wall could also be found

along the edges of the internal walls of these cortical cells. Walls of cortical cells internal to this layer, however, were normal in appearance (Figure 63).

Myriophyllum

Roots of *Myriophyllum* were bound by a layer of small epidermal cells, two layers of hypodermal cells and a single layer of large cortical cells (Figure 64). Epidermal cells appeared collapsed in outline and were eroded away from much of the roots surface. When present, they were characterized by very thin and partially dissolved cell walls and contained electron dense granular material (Figure 66, 67). Cells of the underlining hypodermis were thick-walled and usually consisted of 2 distinct cell types. Cells of the outer hypodermal layer also contained electron dense granular material and showed signs of dissolution along the side facing the epidermis (Figure 66, 67, 68). The internal walls of this layer, however, appeared to be more electron dense than those of the bordering inner hypodermal layer (Figure 68). An examination of this common wall showed that the two hypodermal layers were separated by a distinct electron translucent band which was composed of several fine parallel lamellae (Figure 69). This pattern is characteristic of hypodermal cells walls which contain suberin deposits (Peterson et al., 1978; Robards et al., 1979). A similar layer was also found along the inner tangential and radial walls of the hypodermal cells bordering the cortex (Figure 70). Individual lamellae, however, could not be resolved within this electron translucent band. Cells of the inner hypodermal layer also contained electron dense material which formed hemispherical bodies that lined the periphery of the cell (Figure 68). Neither gas spaces nor plasmodesmata were observed between cells of these layers. Bacteria were also not

observed within the walls of these cells. They appeared to be confined to the outer epidermal region.

Numerous organelles were observed within the underlying layer of cortical cells (Figure 66). They were not found within the hypodermal or epidermal cells (Figure 67, 68). The internal walls of these cells were also examined and did not appear to contain suberin deposits.

Potamogeton

Roots of *Potamogeton* were bound by a single layer of large cortical cells, a layer of thick-walled hypodermal cells and an occasional epidermal cell (Figure 71). Although root hairs were present, most had been sloughed from the root's surface (Figure 71, 72). The outer hypodermal wall was typically covered by a thin layer of electron dense material of unknown origin (Figure 73, 74). Many suberin lamellae were found along the outer edge of this wall (Figure 75). They also appeared to continue down the inner tangential wall and along the inner radial wall which borders underlying cortical cells (Figure 76). The suberin layer divided the wall between these two cells into a lighter hypodermal and darker cortical side (Figure 76). The walls were also impregnated with a substance which produced small electron dense inclusions upon staining (Figure 75, 76). The distribution of these inclusions appeared to be greater within the walls surrounding the cortical cells than in the walls of the hypodermis (Figure 76, 77).

Suberin deposits were not found in the internal walls of the cortical cells. Neither gas spaces nor plasmodesmata were observed between cells of the hypodermis

and cortex. Although numerous bacteria were present of the root surface (Figure 72), they were not found within the walls of these cells.

Lobelia

The root of *Lobelia* was bound by a compact outer layer composed of epidermal, hypodermal and cortical cells (Figure 78, 79). Epidermal cells were small, possessed thin cell walls and were usually collapsed in outline (Figure 79, 80). The underlying hypodermal cells were irregular in shape and possessed a relatively thick outer cell wall (Figure 79). A rather wide electron translucent lamina was found in the middle of this wall, which appeared to completely encircle the cell (Figure 81, 82). This layer was similar to the layer found within the inner hypodermal wall of *Myriophyllum* roots (Figure 70) and may also be composed of suberin. Suberin deposits were not found within the internal walls of the cortical cells. Some of these cells were, however, lined with the wall remains of adjacent cortical cells which collapsed during the formation of lysigenous gas spaces (Figure 83). Cellular organelles were not observed within cells of either the hypodermal or epidermal layers, but were frequently found within the underlying cortical cells (Figure 79, 83). Neither gas spaces nor plasmodesmata were observed between cells of these layers. Bacteria also appeared to be confined to the outer epidermal region of the root (Figure 79, 81).

Figure 58. Cross-section of *Elodea* root. Light micrograph showing size and arrangement of epidermal and cortical cells. Bar=0.1 mm.

Figure 59. Surface of *Elodea* root. SEM micrograph showing epidermal peeling and presence of bacteria. Bar=50 μm.

Figure 60. Epidermis of *Elodea* root. TEM micrograph illustrating outer and inner regions of the outer epidermal wall. Note outer cuticular layer (arrows) and electron translucent lamellae present within the inner region. Bar=1 μm.

Figure 61. Epidermis of *Elodea* root. TEM micrograph showing degradation of outer and anticlinal regions of the epidermal cell (EP) wall. Bar=1 μm.

Figure 62. Cross-section of *Elodea* root. TEM micrograph of junction between epidermis (EP) and underlying cortical (C) cell. Walls are lined with a few electron translucent lamellae (arrows). Bar=1 μm.

Figure 63. Cross-section of *Elodea* root. TEM micrograph showing walls of adjacent cortical cells forming a gas space. Bar=2.5 μm.

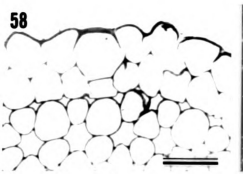
58

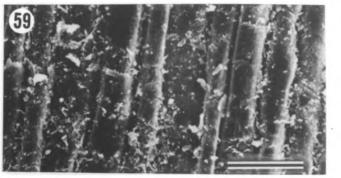
59

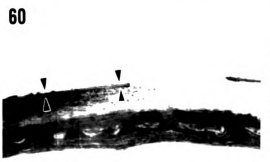
60
EP

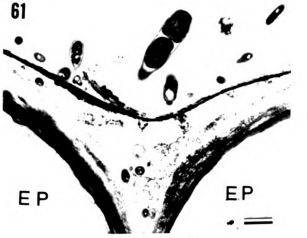
61
EP
EP

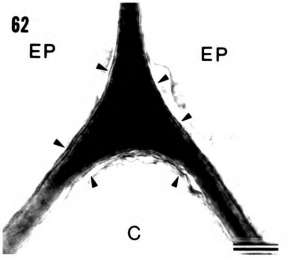
62
EP
EP
C

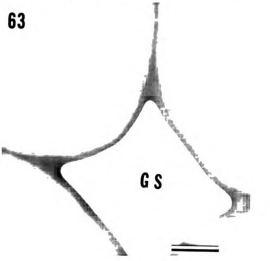
63
GS

Figure 64. Cross-section of *Myriophyllum* root. Light micrograph showing size and arrangement of outer layer of cells. Bar=0.1 mm.

Figure 65. Cross-section of *Myriophyllum* root. TEM micrograph through epidermal (EP), hypodermal (HY) and cortical (C) cells. Bar=5 μm.

Figure 66. Surface of *Myriophyllum* root. SEM micrograph showing epidermal peeling. Bar=20 μm.

Figure 67. Cross-section of *Myriophyllum* root. TEM micrograph showing degrading walls of epidermal (EP) and hypodermal (HY) cells. Bar=2.5 μm.

Figure 68. Cross-section of *Myriophyllum* root. TEM micrograph at junction between hypodermal (HY) and cortical (C) cells. Bar=2.5 μm.

Figure 69. Cross-section of *Myriophyllum* root. TEM micrograph of electron translucent suberin lamellae (arrows) in wall between hypodermal cells. Bar=0.1 μm.

Figure 70. Cross-section of *Myriophyllum* root. TEM micrograph showing band of suberin (arrows) in wall between hypodermal and cortical cells. Bar=2.5 μm.

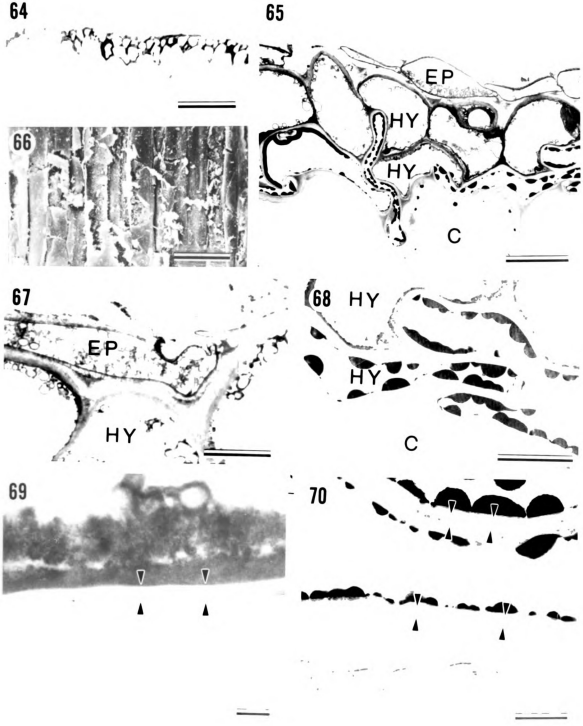
64
65
EP
HY
HY
C
66
67
EP
HY
68 HY
HY
C
69
70

Figure 71. Cross-section of *Potamogeton* root. Light micrograph showing the size and arrangement of outer cell layers. Bar=0.1 mm.

Figure 72. Surface of *Potamogeton* root. SEM micrograph showing root hairs, presence of bacteria and epidermal peeling. Bar=50 μm.

Figure 73. Cross-section of *Potamogeton* root. TEM micrograph through outer layer of root showing hypodermal (HY) and cortical (C) cells. Bar=10 μm.

Figure 74. Cross-section of *Potamogeton* root. TEM micrograph of outer wall of hypodermal cell. Bar=1 μm.

Figure 75. Cross-section of *Potamogeton* root. TEM micrograph of anticlinal wall of hypodermal cell showing suberin lamellae and electron dense inclusions. Bar=0.5 μm.

Figure 76. Cross-section of *Potamogeton* root. TEM micrograph at common wall between hypodermal (EP) and cortical (HY) cell delineated by electron translucent suberin lamellae. (Note abbreviations are mislabeled). Bar=0.5 μm.

Figure 77. Cross-section of *Potamogeton* root. TEM micrograph of cortical (C) cell bordering hypodermis (HY) and lysigenous gas space (GS). Bar=25 μm.

71

72

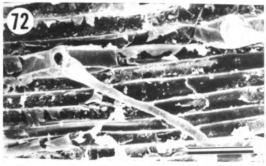

73

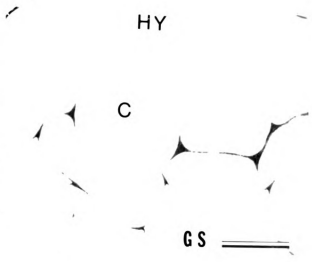

74

75

76

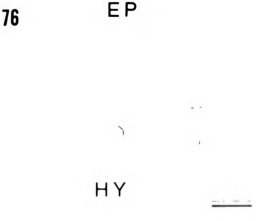

77

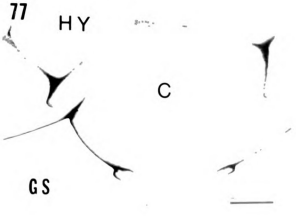

Figure 78. Cross-section of *Lobelia* root. Light micrograph showing size and arrangement of outer layer of cells. Bar=0.1 mm.

Figure 79. Cross-section of *Lobelia* root. TEM micrograph through epidermal (EP), hypodermal (HY) and cortical (C) cells. Bar=5 μm.

Figure 80. Surface of *Lobelia* root. SEM micrograph showing collapsed appearance of epidermal cells. Bar=25 μm.

Figure 81. Cross-section of *Lobelia* root. TEM micrograph showing epidermal (EP) cells and underlying hypodermal cells. Bar=1 μm.

Figure 82. Cross-section of *Lobelia* root. TEM micrograph at junction of hypodermal and cortical cell layers showing thick translucent suberin layers (arrows). Bar=5 μm.

Figure 83. Cross-section of *Lobelia* root. TEM micrograph of inner cortical (C) cell bordering lysigenous gas space (GS) which is lined with remains of collapsed cell walls. Bar=2.5 μm.

78

79

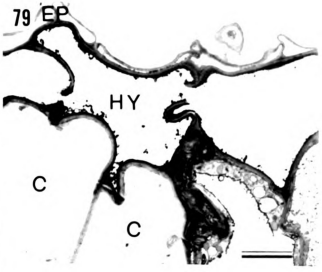

80

81

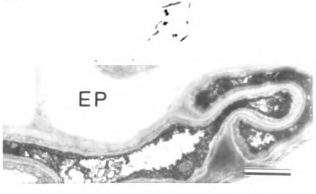

82

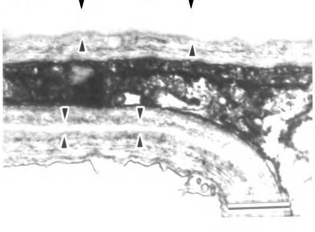

83

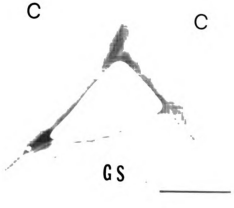

DISCUSSION

Hypodermal cells containing suberin lamellae were found in the roots of *Myriophyllum*, *Potamogeton* and *Lobelia*. Plasmodesmata were not observed between cells of the hypodermis and the epidermal and cortical cells adjacent to this layer. If plasmodesmata are not present in these walls, it is likely that water and ions transported through these cells would have to cross the suberin layer. Suberin is known to form a relatively impermeable barrier which can drastically reduce the rate of transport across the cell wall (Robards et al., 1973; Ferguson and Clarkson, 1977; Robards et al., 1979). Although direct evidence does not exist, it is likely that suberin also restricts the transport of dissolved gases. In the roots of the sand sedge, *Carex arenaia*, the suberized walls of the hypodermal cells are thought to form an effective barrier to radial diffusion of O_2 into the root (Robards et al., 1979). In *Lobelia*, transport of O_2 through the root wall was found to provide substantial resistance to O_2 release (Sand-Jensen and Prahl, 1982). These observations support the interpretation that suberized walls may restrict gas transport across the root. The presence of suberin in the wall does not, however, always indicate a low permeability of the cell to the transport of water or ions (Clarkson et al., 1978; Clarkson et al., 1987). It is not known how the presence or absence of plasmodesmata through the suberin layer of hypodermal cells affects root permeability.

Hypodermal cells were not produced in the roots of *Elodea*. Although electron translucent lamellae were found in the walls of some epidermal and underlying cortical cells, these structures differed in both their appearance and location from the suberin layers observed in hypodermal cells of the other species examined. Since they were

typically found in walls undergoing dissolution, they may represent the degradation product of some wall component.

Suberization of the hypodermal cell wall may not only retard transport across the root, but may also restrict the rate of bacterial invasion within the walls of the internal cells. Roots of *Elodea* do not appear to produce a hypodermal layer and may therefore be more susceptible to the activities of soil bacteria. In these plants, roots are produced adventitiously from the nodes of an upright stem and are often loosely anchored in the sediments. The need for an outer protective layer may not be as great in this species. Roots of *Myriophyllum*, *Potamogeton* and *Lobelia*, however, are produced on an underground stem or rhizome and buried in the sediments and may have an increased need for protection. Although suberization of the hypodermis may increase the resistance of this wall, it must eventually break down, since bacteria and fungi can be found in hypodermal cells and in cortical cells internal to this layer (Kuo et al., 1981).

Roots of *Potamogeton* are often rust-colored and probably contain iron. The unusual speckled staining of inclusions observed in these roots suggests that iron may have precipitated within the cell walls. Large crystals of iron have been identified within the wall of cortical cells of rice roots exposed to anaerobic conditions (Green and Etherington, 1977). In *Spartina*, iron deposits are confined to the wall of epidermal cells (Mendelssohn and Postek, 1984). Iron is soluble in water in its reduced state and is highly mobile within sediments (Ponnamperuma, 1984). The presence of iron within walls of these roots would suggest that at some point in time release of O_2 from the root was reduced to a level which led to a reduction in the thickness of the oxidized layer and the penetration of reduced iron into the root (Armstrong, 1979). The extent to which

iron penetrates the root should therefore reflect both the permeability of the root wall to iron transport and the point at which oxidation and immobilization of iron occurred (Taylor et al., 1984).

The amount of O_2 released by the root is a function of its surface area, its resistance to O_2 diffusion and the difference in O_2 concentration between the lacunar atmosphere of the root and that of the surrounding sediments (Armstrong, 1979). The development of a suberized hypodermal layer in roots may confer two important adaptive advantages. First, it may provide a substantial resistance to the radial loss of O_2 from the roots and thus promote long distance transport of O_2 to the root tip where it is especially needed for growth and development. Many studies which examine gas exchange across the roots assume permeability is uniform along the length of the root (Sand-Jensen and Prahl, 1982; Boston et al., 1987a, 1987b). If the mature root wall is relatively impermeable to gases, then calculations based on total surface area may not accurately measure flux of gases from the roots. Secondly, the hypodermis may also act as a barrier to the entry of phytotoxic compounds. The resistance of this layer may become increasingly significant when, during periods of reduced O_2 availability, a reduction in the oxidative powers to protect the root from the reduced nature of the sediments occurs.

CHAPTER IV

RESISTANCE TO GAS TRANSPORT

INTRODUCTION

O_2 transport to and release from the roots of submersed plants increases dramatically during the light (Sand-Jensen et al., 1982; Carpenter et al., 1983; Smith et al., 1984; Thursby, 1984; Kemp and Murray, 1986). O_2 produced during photosynthesis is therefore thought to provide the major source of O_2 for transport to roots buried in O_2 deficient sediments (Wetzel, 1975; Smith et al., 1988). Submersed plants have been shown to differ in their O_2 transport abilities (Sand-Jensen et al., 1982). These differences may be of both physiological (Penhale and Wetzel, 1983; Smith et al., 1988) and ecological (Carpenter et al., 1983; Smith et al., 1984; Thursby, 1984; Kemp and Murray, 1986) significance.

Gradients of decreasing O_2 concentrations from the shoots to the roots are known to exist within the lacunar atmosphere of aquatic macrophytes (Barber, 1961; Teal and Kanwischer, 1966; Dacey, 1981; Brix, 1988). O_2 transport has been shown to occur down this gradient at rates consistent with gas phase diffusion (Barber et al., 1962; Armstrong, 1964; Sorrell and Dromgoole, 1987). Thus, the lacunar atmosphere of aquatic plants has traditionally been thought of as a static system where gas transport occurs purely by molecular diffusion along established concentration gradients.

Mass flow of gases through the lacunar system, however, has recently been demonstrated in a number of emergent species. Two basic mechanisms have been proposed. One is a flow-through system as described by Dacey (1980, 1981) for waterlilies, which has also been shown to operate in *Phragmites* (Armstrong, 1989). According to this mechanism, pressures develop in young leaves as they heat up during the day. This pressurization generates a mass flow of gases down the petiole, through the rhizome and out older leaves of the plant. The other mechanism proposed by Raskin and Kende (1983, 1985) is based upon a pressure deficit that is generated by the solubilization of respired CO_2 into the water surrounding the plant.

In *Phragmites*, mass flow of O_2 to the roots and rhizomes during the day transports roughly 30 times more O_2 than is capable by diffusion alone (Armstrong and Armstrong, 1988). During the night, when pressure gradients no longer are formed, diffusion becomes significant as steep O_2 gradients develop between the shoots and the roots (Armstrong and Armstrong, 1988; Brix, 1988; Koncalova, 1988).

O_2 produced during photosynthesis preferentially partitions into a gas phase (Sorrell and Dromgoole, 1986). This increases not only the O_2 concentration within the lacunar atmosphere of submersed plants (Hartman and Brown, 1967; Oremland and Taylor, 1977), but also the pressure within the lacunar system (Sorrell and Dromgoole, 1988). Thus the potential for mass flow exists in submersed plants. Little, however, is actually known about the relative significance of mass flow and diffusion with respect to O_2 transport in these plants. Sorrell and Dromgoole (1987) concluded that the rates of O_2 transport they observed from the roots of *Egeria* could be satisfied by diffusion alone.

Smith et al. (1984), on the other hand, report that the O_2 transport rates they observed for seagrasses were greater than that possible by diffusion alone.

The purpose of this study was twofold. First to examine the relationship between lacunar structure and gas transport by estimating the resistances associated with both diffusion and mass flow. And secondly, to evaluate the physiological/ecological significance of the lacunar system by comparing the transport abilities of selected species.

Diffusion of O_2 down a simple stem can most easily be described by Fick's first law (Armstrong, 1979; Sorrell and Dromgoole, 1987) as:

$$J = \frac{\Delta D}{R} \qquad \text{(Equation 1)}$$

where J=flux density ($cm^3\ cm^{-2}\ s^{-1}$) and ΔC = concentration gradient ($cm^3\ cm^{-1}$) and R=resistance of the tissue to diffusion ($s\ cm^{-3}$).

The flux of O_2 down a simple stem by mass flow can be defined by the Hagen-Poiseuille equation (Nobel, 1983; Sorrell and Dromgoole, 1988) as:

$$J = \frac{\Delta P}{R} \qquad \text{(Equation 2)}$$

where ΔP=pressure gradient ($kPa\ cm^{-3}$) and R=resistance per cm to mass flow ($kPa\ s\ cm^{-3}$). Note that in diffusion, the concentration gradient is the driving force, whereas in mass flow, the pressure gradient is the driving force.

Stems of submersed plants are typically divided into nodes and internodes. Lacunae form large gas canals that are continuous throughout the length of the internode, but are interrupted at the node by perforated plates of cells called diaphragms (Chapter II). Resistance (R_I, $s\ cm^{-3}$) of the internode to diffusion is determined by:

$$R_i = \frac{L}{DA} \qquad \text{(Equation 3)}$$

where L=length of the stem segment (cm), D=diffusion coefficient of gas in question ($cm^2\ s^{-1}$) and A=cross-sectional area through which gas is diffusing (cm^2).

Resistance (r_i, kPa s cm^{-3}) of the internode to mass flow is defined as:

$$r_i = \frac{8\eta L}{N\pi r^4} \qquad \text{(Equation 4)}$$

where η=viscosity of lacunar gas (kPa s), N=number of gas lacunae and r=mean lacunar radius (cm). Note that in Equation 3, R_i is a function of the diffusion coefficient of a specific gas, whereas in Equation 4, r_i is a function of η, the viscosity of the lacunar gases. This comparison emphasizes the fact the diffusion is the movement of a specific gas, whereas mass flow is the movement of the bulk gases present.

According to these equations, resistance to transport through the internode can be influenced morphologically by the length of the path and anatomically by the extent of lacunar development. Lacunar structure, however, affects resistances to diffusion and mass flow differently. Diffusive resistance is a function of the total gas space area and is not influenced by the actual number and size of the lacunae (assuming r>than free mean path of gas, Nobel, 1983). Resistance to mass flow, on the other hand, is a function of both the number of lacunae and the 4th power of the radius of the lacunae.

Equations which characterize resistances across the nodal diaphragms are essentially analogous to Equations 3 and 4. Resistance (R_N, s cm^{-3}) of the node to diffusion is determined by:

$$R_N = \frac{l + 2r_p}{Dna_p} \qquad \text{(Equation 5)}$$

where l is the depth of the pore, r_p is the radius of the pore, n is the number of pores across the node and a_p is the average area per pore.

Resistance (r_n, kPa s cm^{-3}) of the node to mass flow is analogous to that of the internode and is determined by:

$$r_n = \frac{8\eta l}{nr_p} \qquad \text{(Equation 6)}$$

where l is the depth of the pore and n is the number of pores across the node. Note again that resistance to diffusion is a linear function of the total gas space area across the node, while resistance to mass flow is an exponential function of the radius of the pore.

RESULTS

Estimates of resistance to both diffusion and mass flow of gases were determined for stems of *Elodea*, *Myriophyllum heterophyllum*, *M. spicatum* and *Potamogeton*. Resistance values are expressed as resistance per cm stem length and are denoted as R (s cm^{-3}) for diffusion and r (kPa s cm^{-3}) for mass flow. Morphological and anatomical data were also collected on the stems and nodes/diaphragms examined. Predicted resistances were calculated using this information and are compared with measured values. Estimates of resistance were used to examine the influence of lacunar structure on diffusion and mass flow and to evaluate the potential significance of these mechanisms to gas transport. The results are organized into two sections in this chapter, namely diffusion and mass flow.

Diffusion

Resistance through nodes.

The influence of nodal tissue on diffusion of gases through the stem was examined by comparing the resistances of stem sections with nodes to sections without nodes. Resistances were measured in stems of three different species, all of a given stem diameter, and in *M. spicatum*, across a range of stem diameters (.12-.24 cm). No significant differences in R were detected between stem types ($\pm$ node) of the three species examined (Table 4). Nodes also appeared to have no measurable effect on R in stems of *M. spicatum* over the range of diameters examined (Analysis of Covariance, $P < .8222$; Table 5).

It was assumed that nodes offered little resistance to diffusion of gases through the stems examined and that the data for both stem types could be pooled for further analysis.

Resistance and gas space.

In *M. spicatum*, porosity values increased with increasing stem diameter (Table 5). Increasing porosity resulted in an increase in the cross-sectional gas space area (A) and a decrease in R (Table 5). R is defined by Fick's first law as L/DA (Equation 3), where D is a constant (ie.- the diffusion coefficient of a given gas). Estimates of R obtained for *M. spicatum* were plotted against 1/DA (Figure 84). R increased as A decreased (r^2=.58). Although the regression of this relationship was highly significant ($P<.0001$), the slope differed significantly from 1 ($P<.05$), thus suggesting that the observed relationship roughly approximates Fick's first law.

Stems of *M. spicatum* are anatomically similar to stems of *M. heterophyllum* (Chapter II). When stems of equal diameter (d=.20 cm) were compared between these two species, significant differences in both porosity and A were found ($P<.05$, Table 6). Lacunae occupied a larger proportion of the cross-sectional area of stems of *M. spicatum*. This increase in A was associated with a significantly lower estimate of R as compared to stems of *M. heterophyllum* ($P<.05$, Table 6). Estimates of R were not significantly different ($P>.05$), however, when stems of different diameters but equal A were compared (Table 6). Differences in both lacunar development and A appeared to account for the observed differences in R between these two species.

Estimates of mean porosity, A, and R of *Potamogeton* and *Elodea* were determined (Table 6). Both porosity and A decreased in order from *Potamogeton*, *Myriophyllum* to *Elodea*. R also increased across species as A decreased. Thus the relationship of R to 1/DA also appears to be consistent across species of different anatomies (Chapter II) as well as within a given species over a range of stem diameters.

Predicted values of R.

Estimates of internodal resistance (R_I) were derived from porosity data according to Equation 3 and calculated for each observation. Measured values of R were plotted against these predicted values (Figure 85). The regression of this relationship was highly significant ($P<.0001$), thus confirming a correlation between measured and predicted values ($r^2=.73$, $n=170$). The slope of this line, however, differed significantly from 1 ($P<.001$). This result questions the accuracy of this method of measurement. The ratio of mean measured R to mean predicted R is listed for each species in Table 6. The mean measured R for all observations combined was 590 which is 1.5 times greater than the mean predicted R of 391. Measured R was over 2.5 times the predicted R for stems of high resistance (*Elodea*), but agreed reasonably well with predicted values in stems of low resistance (Table 6, Figure 85).

Estimates of nodal resistance (R_N) were predicted for each species according to Equation 5 (Table 7). The anatomical data from which these estimates were derived are presented in Appendix II. Estimates of R_N ranged from 13-72 s cm^{-3} among the species examined and tended to increase with increasing values of R_I (Table 7).

The significance of R_N to diffusive gas transport was examined by constructing hypothetical 1 cm stem segments which contain a single node. The relative values for R_N and R_I for this stem were calculated (Table 7). Among the species examined, nodal diaphragms were estimated to account for only 3-15% of the total resistance to diffusion. These findings agree well with the observations of measured resistances in that nodes appeared to have no significant effect on the diffusion of gases through the stem (Table 4).

Resistance and O_2 transport.

With these estimates of resistance, one can, through manipulations of Fick's first law, determine the O_2 gradient necessary to drive a given rate of O_2 transport from the shoots to the roots by diffusion alone. Two estimates of rates of O_2 transport (F) were obtained from the literature. Sorrell and Dromgoole (1987) measured a transport rate of 6.28 μl O_2 h^{-1} (1.74×10^{-6} cm^3 O_2 s^{-1}) for individual stems of *Egeria*. This value corresponded to the rate of O_2 consumption and release by a 5 cm root segment subjected to O_2-depleted water. Sand-Jensen et al. (1982) measured a rate of .50 μg O_2 mg^{-1} plant dry wt h^{-1} for plants of *Potamogeton* under similar conditions. This value was converted into a mean transport rate of 85.5 μl O_2 h^{-1} (2.375×10^{-5} cm^3 O_2 s^{-1}) for a 50 cm stem using 228 mg dry wt per 50 cm shoot as a conversion estimate (Kemp and Murray, 1986). The two rates of O_2 transport are termed LOW and HIGH, respectively.

Under steady state conditions, the rate of O_2 transport from the base of the shoot expressed per unit area is termed the flux density (J, cm^3 O_2 cm^{-2} s^{-1}) and is determined by the transport rate (F, cm^3 O_2 s^{-1}) divided by the cross-sectional area of the stem (cm^2) (Sorrell and Dromgoole, 1987). According to Fick's first law, J is also equal to the O_2

concentration gradient divided by the resistance (Equation 1). Thus the concentration gradient required to meet a specified flux can be determined if the resistance to transport is known. The O_2 concentration of the lacunar atmosphere increases during photosynthesis and can range from 30% (Hartman and Brown, 1967; Oremland and Taylor, 1977; Roberts and Moriarty, 1987) up to 60% O_2 (Sorrell and Dromgoole, 1987). An upper limit of 40% O_2 in the shoots during photosynthesis was arbitrarily chosen and the lower limit assumed to be 0% O_2 surrounding the roots. These conditions set the maximum gradient at 40% O_2. Therefore plants whose estimates of ΔC ($\Delta C = JR$) exceed 40% O_2 cannot transport enough O_2 to the roots by diffusion alone to meet the O_2 demand imposed (LOW or HIGH transport rates). The concentration gradients required to meet both the LOW and HIGH O_2 transport rates (F) were determined for 50 cm stem sections of each species using this relationship and values of R measured and R predicted (Table 6). The results indicate that the LOW rate of O_2 transport could be supported by diffusion alone in all species examined when calculations are based on R predicted (Table 8). *Elodea* is the only exception when ΔC is based on R measured, since the O_2 required to drive diffusion (64%) exceeds the 40% O_2 upper limit. The results also show that only two of these species could supply enough O_2 by diffusion alone to support the HIGH rate of O_2 transport. They are *Potamogeton*, the genus from which the transport rate was determined, and the larger stemmed individuals of *M. spicatum*. Thus resistances encountered along the lacunar pathway are too large in stems of *Elodea*, the smaller stems of M. spicatum, and the less porous stems of *M. heterophyllum* to support the HIGH rate of O_2 transport.

Mass Flow

Resistance through nodes.

The influence of nodes on resistance to mass flow was examined by comparing stem sections with nodes to sections without nodes (Table 9). The presence of a node in the stem section significantly ($P < .05$) increased r in all 3 species examined. In *M. spicatum*, an increase in r was also detected within the different size classes examined ($P < .05$). These values of r were not direct estimates of nodal resistance, since the resistance of the node was expressed on a per cm stem basis. The data were further analyzed to determine an estimate of nodal resistance by subtraction of the internodal resistance from the total resistance measured.

Internodal resistance (r_i, kPa s cm^{-3}), the resistance to longitudinal transport through the stem lacunae, was examined in *M. spicatum* and *M. heterophyllum* (Table 10). No significant differences between size classes of *M. spicatum* stems or between the 2 species were detected ($P > .05$). Estimates of r_i could not be measured in *Elodea* and *Potamogeton*. Internodes of *Elodea* were too short and delicate to handle without damaging. Internodes of *Potamogeton* are interrupted by diaphragms throughout their length (Chapter II). Thus measurements of r_i for this species also included the resistance associated with these structures.

Values of r_i were predicted for each species using Equation 4 (Table 10). The anatomical data from which these estimates are derived is given in Appendix II. Predicted values were very low (.02-.13) in both *Myriophyllum* species. They were, however, from 1 to 2 orders of magnitude lower than the measured values for these

stems. The differences between measured and predicted values may represent problems associated with detecting a relatively low resistance. The large confidence interval associated with these measurements supports this interpretation. Stems of *Elodea* were characterized by the smallest lacunar radius (Appendix II) and had a relatively large predicted r_i (3.14).

Estimates of nodal resistance (r_n, kPa s cm^{-1}) were obtained by subtracting r_i from r, total resistance measured. For *Potamogeton* and *Elodea*, predicted values of r_i were multiplied by 10 to adjust for measurement discrepancies. An estimate of internodal diaphragm resistance (r_d) for *Potamogeton* was first determined by subtracting predicted r_i from the r of stem sections without nodes and determining a mean r_d by dividing this value by the number of diaphragms present. The mean r_d calculated was then multiplied by the number of diaphragms present in the nodal section. This value represented the total resistance attributed by the diaphragms. r_n was then estimated by subtracting this value from r.

Measured estimates of r_n ranged from 4 to 203 kPa s cm^{-3} among the 4 species examined (Table 10). r_n was lowest in *M. heterophyllum* and increased from *M. spicatum*, *Potamogeton* to *Elodea*. In *M. spicatum*, a nearly 5-fold difference in r_n was detected between the smallest (66 kPa s cm^{-3}) and largest (14 kPa s cm^{-3}) nodes examined ($P < .05$).

Values of r_n were predicted for each species using Equation 6 (Table 10). The anatomical data from which these estimates were derived is presented in Appendix II. Predicted estimates were typically within an order of magnitude of the measured values but ranged from 10% to nearly 300%.

The relative resistance of nodes and internodes to mass flow was evaluated by constructing hypothetical 1 cm stem sections containing a single node. Of the species examined, nodes accounted for 87-97% of the measured resistance (Table 10). Resistance through the internodes was relatively insignificant (3-8%) in all species except in *Elodea* (13%).

The total resistance to mass flow was estimated for 50 cm sections of stems for each of the 4 species examined using measured estimates of r_n and predicted estimates of r_i (Table 10). Since nodes and internodes are constructed in series, their resistances are directly additive. Total resistance (r_t, kPa s cm^{-3}) was calculated as the sum of r_n times the number of nodes estimated for a 50 cm stem and r_i expressed over the 50 cm length of the stem (Table 11). Estimates of total resistance for a 50 cm stem ranged from 300 to 13,770 among the species examined. The lowest r_t was determined for *Potamogeton* and the highest for *Elodea*. In stems of *M. spicatum*, a relatively small decrease in stem diameter resulted in a nearly 5 fold increase in the total resistance of the pathway. In *Potamogeton*, r_n was determined to be roughly 30 times greater than r_d (Table 10). In the stems examined, there were 8 ± 1 (n=60) diaphragms visible per internode. Internodal diaphragms accounted for only 17% of the total resistance to mass flow, the remaining 83% attributable to the node (Table 11) since resistance through the lacunae themselves (without diaphragms) was predicted to be insignificant (Table 10).

Mass Flow and O_2 transport.

The rate of transport (F, cm^3 s^{-1}) through a stem by mass flow is defined by the Hagen-Poiseuille equation (Equation 2) and is equal to the pressure gradient along a

given length of stem (kPa) divided by R (kPa s cm^{-3}), the total resistance encountered in the pathway. Given a specific O_2 transport rate (F), one can, using this equation, determine the pressure gradient required to support that flow rate. Estimates of LOW and HIGH O_2 transport rates used in the analysis of diffusion (Table 8) were adjusted to account for mass flow of bulk gases. The lacunar atmosphere was again assumed to be 40% O_2, thus rates were multiplied by 100/40 = 2.5 to account for transport of bulk gases and not just O_2. The ΔP required to support both LOW (4.35×10^{-6} cm^3 gas s^{-1}) and HIGH (5.94x10-5 cm3 gas s-1) rates of O_2 transport are given in Table 11. Estimates of ΔP are very low for *Potamogeton*, *M. heterophyllum* and the larger stems of *M. spicatum* and relatively very large in *Elodea*. Stems of *Elodea* would require a pressure gradient 5-60 times larger than the other species examined in order to acheive the same flux rate.

Table 4. A comparison of the measured diffusive resistance (R, s cm^{-3}) of stem sections, with and without nodes, of three species. Data are presented as mean ± 95% confidence interval (number of measurements). NSD denotes no significant difference between stem types (P > .05).

Species	Stem diameter (cm)	Diffusive resistance (R, s cm^{-3}) with node	Diffusive resistance (R, s cm^{-3}) without node
M. spicatum	.20	212 ± 114 (13)	311 ± 168 (6) NSD
M. heterophyllum	.20	796 ± 296 (16)	659 ± 292 (16) NSD
Potamogetom	.24	184 ± 76 (18)	229 ± 89 (13) NSD

Table 5. Statistical analysis of stems of *M. spicatum*. 1. The effect of stem type (± node) and stem radius on diffusive resistance (R, s cm^{-3}). 2. Regression of porosity, gas space and R on stem radius.

1. Analysis of Covariance:

Model	R = stem type + radius	
Variable	stem type ($P < .8222$) radius ($P < .0001$)	

2. Regression:

Porosity	2.43 radius + 29	($r^2 = .68$, n = 98)
Gas space	.37 radius - .02	($r^2 = .89$, n = 98)
R (s cm^{-3})	-14604 radius + 1772	($r^2 = .43$, n = 98)

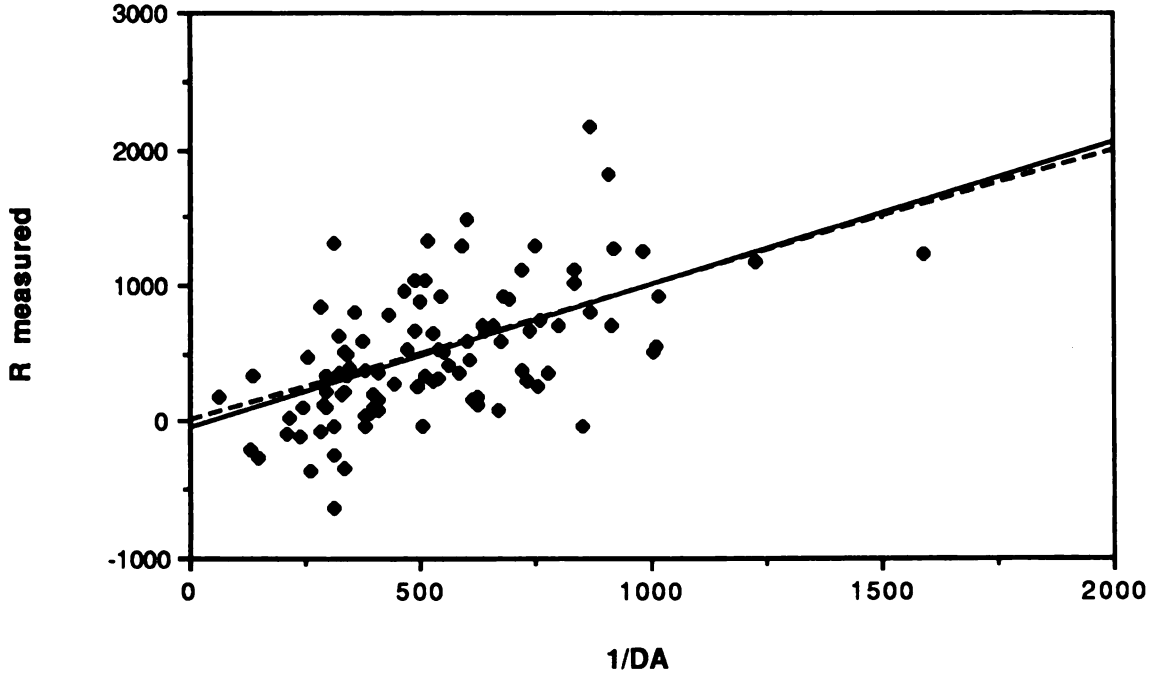

Figure 84. Regression of resistance per cm stem (R, s cm^{-3}) on 1/DA (s cm^{-3}). The dotted line with slope of 1 indicates R=1/DA in accordance with Fick's first law. The solid line is a regression through data points (slope=1.22; r^2=.56; n=98).

Table 6. Diffusive resistances to gas transport. Values obtained by direct measurement and by prediction using Fick's First Law and estimates of porosity and gas space area of 4 species. Data are presented as mean ± 95% confidence interval (number of measurements). Specific contrasts were performed between classes of *Myriophyllum*. Different lower-case letters within a column indicate significance between contrasts ($P < .05$) based on Scheffe's Interval Test (Gill, 1978).

Species	Stem diameter (cm)	Porosity	Gas space (cm^2)	Rmeasured ($s\ cm^{-3}$)	Rpredicted ($s\ cm^{-3}$)	Rmeasured / Rpredicted
M. spicatum	.16	.498 ± .013 (24)a	.012 ± .001 (24)a	515 ± 156 (24)ab	416 ± 25 (24)a	1.2
	.20	.522 ± .015 (20)b	.018 ± .001 (19)b	244 ± 82 (19)b	303 ± 29 (19)b	.8
M. heterophyllum	.20	.346 ± .009 (26)c	.011 ± .001 (26)a	752 ± 248 (24)a	441 ± 35 (24)a	1.7
Potamogeton	.24	.658 ± .026 (35)	.039 ± .001 (35)	203 ± 57 (31)	132 ± 6 (31)	1.5
Elodea	.12	.248 ± .029 (8)	.003 ± .001 (8)	7353 ± 1117 (7)*	1931 ± 256 (7)*	3.8

*estimate based on assumption that nodes offer no measurable resistance to diffusion.

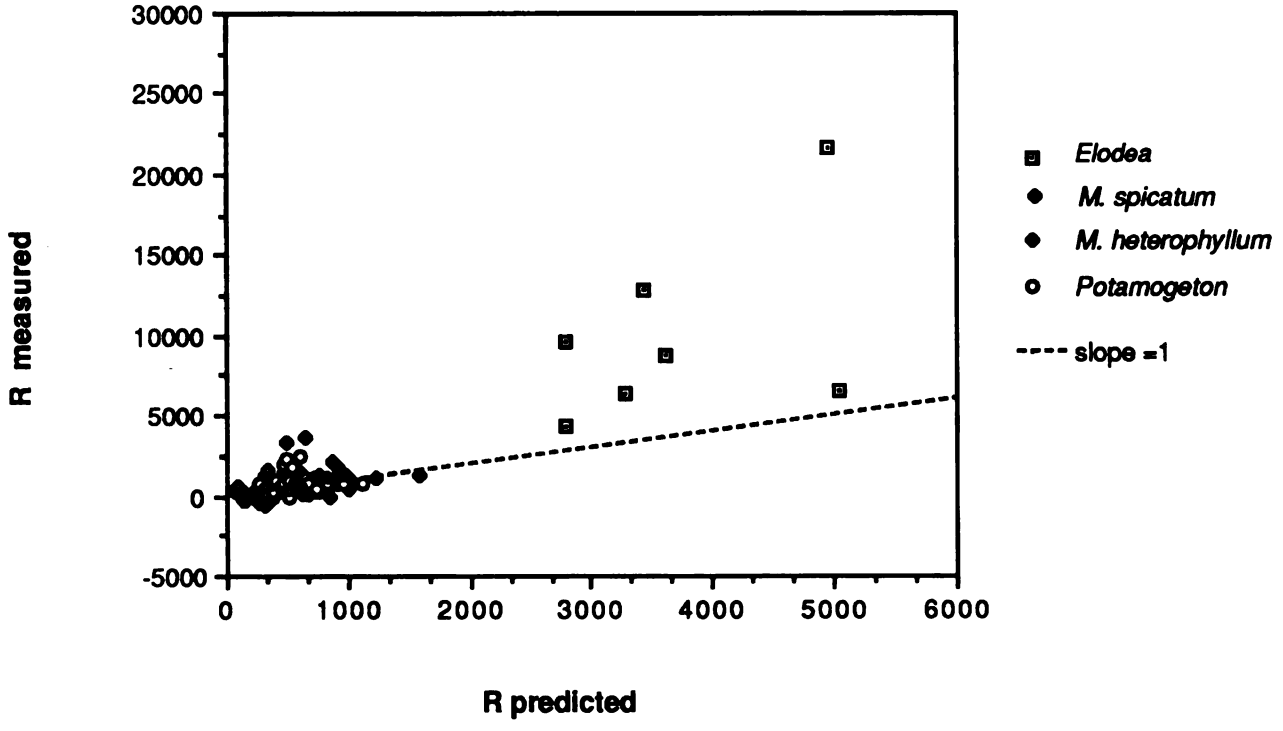

Figure 85. Comparison of measured versus predicted diffusive resistance of stems of four species examined. The dotted line with slope of 1 indicates predicted=measured.

Table 7. Predicted estimates of resistance of nodes (R_N) and internodes (R_I) to diffusion. Estimates of R_I are repeated from Table 3. Estimates of relative resistances are based on hypothetical 1 cm stem sections containing a single node.

Species	Stem diameter (cm)	Resistance (s cm^{-3})		Relative Resistance	
		Node R_N	Internode R_I	Node	Internode
M. spicatum	.16	72 ± 40 (9)	416 ± 25	.15	.85
	.20	13 ± 3 (9)	303 ± 29	.04	.96
M. heterophyllum	.20	36 ± 26 (6)	441 ± 35	.08	.92
Potamogeton	.24	6 ± 1 (9)	132 ± 6	.04	.96
Elodea	.12	66 ± 42 (9)	1931 ± 256	.03	.97

Table 8. Evaluation of resistance to diffusion. Estimates of 0_2 gradients (ΔC, in $\%O_2$) required to support the given transport rate by diffusion alone through 50 cm stem sections of four species. LOW and HIGH transport rates are 1.74×10^{-6} and 2.375×10^{-5} cm^3 0_2 s^{-1}, respectively (see text). 0_2 gradients based on both measured and predicted resistances. * denotes situations where transport rate is satisfied given an upper limit to ΔC of 40% 0_2 (see text).

			LOW Transport Rate (F)			HIGH Transport Rate (F)		
				Rmeasured[b]	Rpredicted[b]		Rmeasured[b]	Rpredicted[b]
Species	Stem radius (cm)	Stem cs. area (cm^2)	J[a] cm^3 0_2 cm^{-2} s^{-1}	ΔC ($\%0_2$)	ΔC ($\%0_2$)	J[a] cm^3 0_2 cm^{-2} s^{-1}	ΔC ($\%0_2$)	ΔC ($\%0_2$)
M. spicatum	.08	.020	8.7×10^{-5}	4.7*	3.8*	1.2×10^{-3}	64.4	52.5
	.10	.031	5.6×10^{-5}	2.2*	2.8*	7.7×10^{-4}	30.5*	38.0*
M. heterophyllum	.10	.031	5.6×10^{-5}	6.9*	4.0*	7.7×10^{-4}	94.0	55.4
Potamogeton	.12	.045	3.9×10^{-5}	1.8*	1.2*	5.3×10^{-4}	25.4*	16.6*
Elodea	.06	.011	1.6×10^{-4}	64.0	17.9*	2.2×10^{-4}	873.0	246.0

[a] J=flux density of 0_2 (cm^3 0_2 cm^{-2} s^{-1}) determined by F/stem area (see text).

[b] ΔC determined by multiplying J by estimates of R (both measured and predicted) from Table 3, adjusted to the diffusion coefficient of 0_2 ($Dch_4/Do_2 = 1.05$) multiplied by the cross-sectional area of the stem and expressed over a 50 cm length (R, s cm^{-1}).

Table 9. A comparison of the measured resistance to mass flow (r, kPa s cm^{-3}) of stem sections, with and without nodes, of three species. Data are presented as mean ± 95% confidence interval (number of measurements). *denotes significant difference between stem types ($P < .05$ - $P < .0001$).

Species	Stem diameter (cm)	Resistance to mass flow (r, kPa s cm^{-3}) with node	Resistance to mass flow (r, kPa s cm^{-3}) without node
M. spicatum	.16	45.6 ± 13.8 (15)	2.1 ± 0.8 (13) *
	.20	9.6 ± 18.9 (7)	1.3 ± 0.8 (14) *
M. heterophyllum	.20	4.6 ± 1.0 (16)	0.3 ± 1.0 (7) *
Potamogetom	.24	11.0 ± 1.8 (15)	2.9 ± 1.6 (20) *

Table 10. Resistances to mass flow of internodes and nodes. Estimates obtained by direct measurement and by prediction using Hagen-Poiseuille equation of four species. Data are presented as mean ± 95% confidence interval (number of measurements). Estimates of relative resistances are based on Rmeasured and Rpredicted in ( ) for hypothetical 1 cm stem sections containing a single node. Predicted values obtained from Appendix II.

Species	Stem diameter (cm)	Internodal Resistance (r_i, kPas cm^{-3})			Nodal Resistance (r_n, kPas cm^{-3})			Relative Resistance	
		Rmeasured	Rpredicted	Rmeasured / Rpredicted	Rmeasured	Rpredicted	Rmeasured / Rpredicted	Node	Internode
M. spicatum	.16	2.13 ± 0.80 (13)	0.13	16.4	66 ± 24 (13)	138	.5	.97 (100)	.03 (0)
	.20	1.25 ± 0.80 (13)	0.02	62.5	14 ± 33 (7)	5	2.8	.92 (100)	.08 (0)
M. heterophyllum	.20	.35 ± 1.00 (17)	0.05	7.0	4 ± 2 (15)	55	.1	.92 (100)	.08 (0)
Potamogeton	.24		0.04		31 ± 7 (15)				
diaphragm					1 ± .5 (20)	8	.9		
Elodea	.12		3.14		203 ± 66 (8)	69 ± 39 (9)	2.9	.87 (.96)	.13 (.04)

Table 11. Evaluation of resistance to mass flow. Summation of resistances of nodes (r_n, measured) and internodes (r_i, predicted) along 50 cm stem for 4 species examined. Estimation of pressure differential required to meet LOW and HIGH 0_2 transport rates by mass flow alone (see text).

Species	Stem diameter (cm)	# Nodes per stem	Sum r_n	Sum r_i	Sum r_t	LOW Transport Rate ΔP kPa 50 cm^{-1}	HIGH Transport Rate ΔP kPa 50 cm^{-1}
M. spicatum	.16	50	3,300	6	3,306	.014	.196
	.20	50	700	1	701	.003	.042
M. heterophyllum	.20	100	400	1	401	.002	.024
Potamogeton	.24						
node		8	248	2	300	.001	.018
diaphragms		50*	50				
Elodea	.12	67	13,600	170	13,770	.060	.818

*based on x = 8 ± 1 (n = 60) visible diaphragms per internode and an internode length of 6 cm.

DISCUSSION

Nodal and internodal resistance.

Gases were transported down the stem through large gas canals that were continuous throughout the length of the internode (Chapter II). These canals were interrupted at the node, and in *Potamogeton* throughout the internode as well, by finely perforated diaphragms through which gases must pass. Although the gas phase is continuous across the pores of the diaphragm, the pores examined in this study were relatively small (2-5 μm in diameter) and occupied only minor fraction of the total cross-sectional area (.015-.061) of the diaphragm. Studies were therefore to examine the effect of pores on the resistance to gas transport.

Diaphragms had a significant impact on the rate at which gases can be transported through the stem. In hypothetical 1 cm stem sections containing a single node, the node accounts for roughly 3-10% of the total resistance to diffusion and 87-97% of the total resistance to mass flow. Although the porosity of the stem decreased dramatically at the node, diffusion did not appear to be severely affected. This was likely due to the relatively short pathlength through the diaphragm (1-10 μm, estimated). Resistance to mass flow, however, is an inverse function of the radius of the pore to the fourth power. Thus as the radius of the pore decreases, the resistance increases exponentially.

Since nodes had relatively little effect on diffusion, the resistance to transport becomes largely a function of the porosity of the stem and the length of the diffusive path. In mass flow, where most of the resistance was determined by the nodes, the overall resistance of the stem becomes largely a function of the numbers of nodes

distributed throughout the length of the stem. These two mechanisms are discussed separately in later sections.

Review of methods.

The mean measured resistance (R) to diffusion was 1.5 times greater than the mean predicted R. In stems of relatively low resistance, values of measured R were in close agreement with predicted values. In stems of high resistance, as in *Elodea*, the measured values of R were nearly 4 times greater than the predicted R. Although the resistance of nodes of *Elodea* were not examined directly, they were predicted to provide little resistance. It is not clear why measured values were larger than predicted for this species.

Stems of aquatic plants were easily susceptible to damage. It is likely that cutting of the stem segment results in rupture of cells and the blockage of gas canals. Since diffusion of gases occurs 10,000 times slower in water than air (Leyton, 1975), flooding of gas lacunae would result in less gas transported and an overestimation of the resistance. Gas transport can be completely blocked in flooded stems of *Potamogeton* infested with chironomid larvae (Appendix III). Such damage to the plant may have a significant impact on gas transport throughout the plant body.

In *Phragmites*, Armstrong and Armstrong (1988) occasionally found sections of rhizome with unusually low transport capabilities. This was apparently due to the production of callus-like wound tissue or "tylosoids", which drastically increased resistance across the node. Occasionally stem sections were also found in this study with

uncharacteristically high resistances. These stems were not examined. It is not known whether a similar type of wound tissue is also produced in stems of submersed plants.

Predicted esitmates of internodal resistance to both diffusion and mass flow were based on anatomical observations of fresh tissue. Measured estimates were of the same order of magnitude as predicted estimates. Predicted estimates of nodal resistance were based on anatomical observations from SEM photographs taken of nodes that were fixed, dehydrated and critical point dried. Although this process shrank the stem tissue (Appendix II), measured estimates of resistance were also within an order of magnitude of predicted estimates corrected for shrinkage.

Porosity and diffusion.

The results presented in Chapter II support the claim that the lacunar system occupies a significant, yet variable, proportion of the total plant body (Sculthorpe, 1967; Wetzel, 1975). Porosity values were found to increase for both stems and roots from *Elodea*, *Myriophyllum* to *Potamogeton*. The purpose of this section was to establish the relationship between these differences in lacunar development and their resistance to gas transport.

As the gas space area of the stems examined increased, resistance to diffusion decreased. The observed relationship closely approximated Fick's first law (Equation 3) and was valid across species as well as across stem diameters. Resistances varied widely among species and increased from *Potamogeton*, *M. spicatum*, *M. heterophyllum* to *Elodea*. Thus according to Fick's first law, the ability of these species to transport O_2

by diffusion should decrease in this order. The significance of these differences in resistance with respect to O_2 transport to the roots are evaluated in the following section.

Diffusive resistance and O_2 transport.

Estimates of R_N (6 s cm^{-3}) and R_I (249 s cm^{-3}) reported by Sorrell and Dromgoole (1987) for *Egeria densa* are of the same magnitude as the species examined here. The LOW O_2 transport rate used in the preparation of Table 5 was taken from their work and represents the rate of O_2 released and respired by a 5 cm section of *Egeria* root exposed to O_2 depleted water. The authors calculated a concentration gradient equivalent to 2.7% O_2 over a 50 cm stem in order to meet this rate. Since lacunar O_2 concentrations are often over 50% during photosynthesis and the concentration gradient necessary to satisfy this rate was much less than that (2.7%), they concluded that the rate of O_2 transport to the roots could be supported by diffusion alone.

Stems of *Egeria* and the 4 species examined here are typically at least 1 m long. Most of the young healthy leaves are concentrated at the shoot apex, leaves decline in vigor towards the base of the shoot. In addition light is also attenuated down through the water column, thus concentrating photosynthesis at the shoot apex. A 50 cm segment of stem tissue was approximated to represent the base of the stem where O_2 contributions to the lacunar atmosphere would be low. Calculations presented in Tables 5 and 7 are based on this length, thus ΔC occurs across this distance.

Elodea is very similar to *Egeria* in growth form. Both produce segmented stems with whorls of small-lanceolate leaves and adventitious roots at the nodes. The biggest difference between the *Egeria* examined by Sorrell and Dromgoole (1987, 1988) and the

Elodea examined here is stem diameter, .30 cm and .12 cm respectively. Porosity values for these species were essentially equal, .23 and .25, respectively. The predicted R_I for *Elodea* (1931 s cm^{-3}), however, is 6 times greater than that for *Egeria* (311 s cm^{-3}). Since ΔC is proportional to resistance, *Elodea* would require an O_2 gradient 6 times greater than *Egeria* to satisfy the same rate of O_2 transport into the roots.

Setting the upper limit to the O_2 gradient within the lacunar atmosphere at 40%, all species examined, including *Elodea*, would be able by diffusion alone to satisfy the LOW transport rate. The LOW O_2 transport rate was determined for *Egeria* (Sorrell and Dromgoole, 1987) and also may apply to the small rooting biomass of *Elodea*. The other species examined, however, have much larger rooting systems and are likely to have higher O_2 transport requirements. The HIGH O_2 transport rate used in preparation of Table 5 is an average for 5 *Potamogeton* species examined by Sand-Jensen et al. (1982). Of all species examined, only *Potamogeton* and the large stemmed *M. spicatum* would be able to transport enough O_2 to the roots to satisfy this rate. Thus *Elodea*, the small stemmed *M. spicatum* and *M. heterophyllum* would not be able to support this rate by diffusion alone or would require steeper (higher) O_2 gradients than the upper limit of 40% O_2. Based on similar calculations, the Egeria examined by Sorrell and Dromgoole (1987) would require a 37% O_2 gradient, which approaches this upper limit. The 40% upper limit was chosen as an estimate of the average O_2 concentration within the lacunar atmosphere during active photosynthesis. Reported values range from 30% (Hartman and Brown, 1967; Oremland and Taylor, 1977; Roberts and Moriarty, 1987) to 60% O_2 (Sorrell and Dromgoole, 1988). The lacunar O_2 concentration is dynamic, however, and reflects the photosynthetic rate of the plant and therefore undergoes large

diurnal fluctuations. Hartman and Brown (1967) report a lacunar concentration of 10% for *Elodea* during the night; Oremland and Taylor (1977) report a value of 8% for seagrasses. If the upper limit to the O_2 gradient is set at 10%, all species except *Elodea*, would be able to transport O_2 to the roots by diffusion alone at the LOW O_2 transport rate. *Elodea*, the species examined for which this rate may apply would not (17.9% required). None of the species examined would be able to satisfy the HIGH rate of O_2 transport given a 10% upper limit to the O_2 gradient. Even at atmospheric equilibrium (21% O_2) only *Potamogeton* would be able to transport enough O_2 to the roots by diffusion alone to sustain this rate.

The HIGH O_2 transport rate includes O_2 released from the roots and O_2 utilized in root respiration. Root respiration alone accounts for roughly 68% of this rate (Sand-Jensen et al., 1982). Reducing the transport rate by this amount (multiply ΔC in Table 5 by .68) indicates that only *Potamogeton* could support the respiratory rate of the roots, given an upper limit of 21% O_2. It could not meet this rate at a lacunar concentration of 10% O_2, which is an estimate of the lacunar O_2 concentration during the night. These calculations suggest that during low or non-photosynthetic periods, plants with high internal resistances and long diffusion pathways would not be able to transport enough O_2 to the roots to support high rates of respiration and/or O_2 release.

Smith et al. (1988) found that in seagrasses, O_2 transport to the roots was sufficient to sustain aerobic respiration during high rates of photosynthesis. The roots undergo anoxia/hypoxia, however, throughout the night or during periods of low photosynthesis. Not only do roots undergo anaerobic metabolism during this period (Smith et al., 1988; Penhale and Wetzel, 1983), but there is also a decline in the amount

of O_2 released from the roots (Oremland and Taylor, 1977; Smith et al., 1984). This decline leads to a decrease in the thickness of the oxidized rhizosphere surrounding the roots and an increase in the exposure to potentially toxic compounds in the sediments (Chapter III).

The results presented here are consistent with Fick's first law of diffusion (Armstrong, 1972; 1979). As the gas space area of the stem increases, resistance to diffusion decreases. Since diaphragms at the nodes are relatively insignificant to the overall resistance of the transport pathway, the ability of the plant to transport gases throughout the stem becomes largely a function of the porosity of the stem and the pathlength for diffusion. The significance of this relationship becomes apparent when one compares the relative transport abilities of plants with different porosities. For example, small stems of *M. spicatum* would not be able to satisfy the same O_2 demand by the roots as the larger stemmed individuals. This pattern is also observed when a comparison is made between *M. spicatum* and *M. heterophyllum* with stems of equal diameter. The lacunar system of *M. spicatum* is able to transport more O_2 to the roots than the less porous lacunar system of *M. heterophyllum*. The O_2 transport rates from which these comparisons were made are within physiological limits for submersed plants. Thus the small differences in porosity and resistance observed between the plants examined may be of considerable physiological as well as ecological significance. These findings are further discussed within the final summary.

Mass Flow and O_2 Transport

Estimates of r_i (.42 kPa s cm^{-3}) and r_a (3.882 kPa s cm^{-3}) reported by Sorrell and Dromgoole (1988) for *Egeria* are of similar magnitude as those measured/predicted in this study. The resistance summed over a 50 cm stem with an internodal distance of 0.8 cm is equal to 265 kPa s cm^{-3}. This value is less than similar values determined for the species examined in this study. It is 50 times less than that measured and 18 times less than that predicted for *Elodea*.

The gradient required to meet the LOW O_2 transport rate by mass flow alone can be calculated by the Hagen-Poiseuille equation, $\Delta P = FR$ (Equation 2). Both LOW and HIGH transport rates (F) were adjusted (see results) to account for mass flow of bulk gases. The pressure gradient (ΔP) required to meet this rate is equivalent to .001 kPa over a 50 cm section of stem. Actual gradients measured after the onset of photosynthesis were .9 kPa m^{-1} or .5 kPa per 50 cm stem (Sorrell and Dromgoole, 1988). Since measured gradient (.5 kPa) is greater than that calculated (.001 kPa) as necessary, mass flow of O_2 is likely to occur during this phase. At the ΔP observed for *Egeria* (.5 kPa, Sorrell and Dromgoole, 1988) all 4 species examined would be capable of supporting the LOW 0_2 transport rate. All species, except *Elodea*, would also be capable of supporting the HIGH O_2 transport rate by mass flow.

Pressure gradients generated by *Egeria* after the onset of photosynthesis equilibrate rapidly (rate = 0.02 m s^{-1}, Sorrell and Dromgoole, 1988). Therefore even though mass flow may occur during the equilibration period, its duration will be relatively short. Changes in the environment, such as water velocity, light intensity and temperature, may temporarily induce mass flow by generating pressure gradients along

the length of the stem. The pressure gradient established, however, is likely to equilibrate rapidly, thus reducing the time and potential significance of mass flow to O_2 transport.

Equilibration of pressures is not a mechanism for sustained mass flow. For mass flow to operate continuously, a pressure differential must be maintained. Since the pressure gradients required to induce mass flow are relatively small, it may be possible that a decline in the photosynthetic rate along the length of the stem would be sufficient to generate and sustain a pressure gradient. I would suggest that this may have more significance in stems with higher resistances, since a pressure gradient would not equilibrate as rapidly. This hypothesis would be very difficult to examine. One would have to discriminate between mass flow and diffusion, and therefore would need to measure ΔP as well as ΔC. The total volume of gases in stems of submersed plants is relatively small, on the order of 1-4 ml. Thus sampling even 0.1 ml of the lacunar gas would dramatically alter the pressure. Additional problems may also be associated with detecting the rather small pressure differentials required to generate mass flow.

Pressure differentials could also be induced in aquatic plants by the solubilization of respired CO_2 from the roots according to the mechanism described by Raskin and Kende (1983, 1985). Since this mechanism does not require thermal inputs, mass flow could occur during both the day and night. Recent doubt has been shed on the significance of this mechanism for plants growing in aquatic sediments. Aquatic sediments are typically rich in CO_2 and reverse gradients into the roots are commonly observed. This can result in net CO_2 diffusion into the plant, thus preventing mass flow (Raskin and Kende, 1985; Koncalova, 1988). Another concern is that as CO_2 is released

from the root, concentration gradients develop around the root. In this situation, mass flow then becomes regulated by the diffusion of CO_2 away from the root (Beckett et al., 1988). If this mechanism occurs in submersed plants, it is likely to be of little significance to O_2 transport since roots of these plants typically undergo anoxia during the night (Smith et al., 1988), when this mechanism should still be operable.

In the waterlily *Nuphar*, pressure differentials are created between young and old leaves (Dacey, 1980, 1981). Pressures are produced within young leaves across small pores in the mesophyll and are generated due to gradients in temperature and water vapor (Dacey, 1980, 1981; Schröder et al., 1988). Porosity of the leaf increases with age, thus decreasing the leaf's ability to pressurize. The increasing pressure in the leaf is transmitted down the petiole through the rhizome and out the old leaves which serve as vents. This flow-through mechanism also appears to apply to the emergent species, *Phragmites* (Armstrong and Armstrong, 1989). In this rhizotomatous plant, pressures are generated in young culms and are vented out old culms. Although it has not been examined, it is difficult to imagine how a mechanism that is dependent on thermal inputs, such as this one, could operate in submersed plants given the high thermal conductivity of water.

Since pressurization occurs within these plants during photosynthesis (Sorrell and Dromgoole, 1988), a mechanism for mass flow exists. However, if mass flow is to be of any duration, a pressure gradient must be sustained for an extended period of time. *Potamogeton illinoensis* is a rhizotomatous submersed plant that produces a small spike of flowers which emerges up through the water column. These structures may provide a means of venting pressures which build up in the plant (Appendix III). Thus a pressure

differential may develop between young pressurized stems and the stems with emergent flowers in a manner analogous to the flow-through system described for waterlilies (Dacey, 1980, 1981).

FINAL SUMMARY

Although roots of submersed vascular plants usually comprise around 10% of the total plant biomass, much variation exists (Westlake, 1965). Among submersed species, *Lobelia* and *Elodea* probably represent the high and low extremes of the rooted condition. Since submersed plants are capable of taking up nutrients from both the leaves and the roots (Denny, 1972), the amount of roots a given species produces may reflect the degree to which it depends on the sediments as a source of nutrients (Hutchinson, 1975). This would suggest then that in *Lobelia*, most of the nutrients are supplied by the sediments and are taken up by the roots, while in *Elodea*, most of the nutrients are supplied from the water column and are taken up across the leaves. *Potamogeton* and *Myriophyllum* are intermediate in their root production and may utilize both the sediments and the surrounding water as sources of nutrients (Barko, 1983).

The availability of nutrients in the sediments increases as the organic content of the sediments increases (Wetzel, 1975; Ponnamperuma, 1984). Increasing the organic content of the sediments also increases the O_2 demand of the sediments. This results in an increase in the O_2 gradient across the roots buried in these sediments and consequently an increase in the amount of O_2 released by the roots (Armstrong, 1964; 1979; Yamasaki and Saeki, 1979; Brix, 1989; Weisner and Graneli, 1989). Increasing the organic content of the sediments has been shown to reduce the growth and vigor of submersed

plants (Barko and Smart, 1983; Carpenter et al., 1983). It is thought that a high O_2 demand in the sediments may inhibit growth by exceeding the plants ability to transport sufficient O_2 to meet this increase in demand (Barko and Smart, 1983; Carpenter et al., 1983).

The amount of O_2 transported to and released from the roots of submersed plants increases dramatically in the light (Sand-Jensen et al., 1982; Sand-Jensen and Prahl, 1982; Carpenter et al., 1983; Smith et al., 1984; Kemp and Murray, 1986; Sorrell and Dromgoole, 1986; 1987; 1988). It is therefore thought that photosynthesis provides the major source of O_2 for transport in these plants (Sculthorpe, 1967; Wetzel, 1975; Smith et al., 1984; Smith et al., 1988). In seagrasses, enough O_2 is transported to the roots/rhizomes during periods of active photosynthesis to sustain aerobic metabolism. During the night or periods of reduced photosynthesis, the O_2 concentration within the lacunar atmosphere decreases dramatically, thus reducing the amount of O_2 available for transport (Oremland and Taylor, 1977; Sand-Jensen et al., 1982; Smith et al., 1984; Smith et al., 1988). Uptake of O_2 from the water is often difficult. Not only is the O_2 concentration frequently low in the water surrounding the plant, but it also diffuses at a rate 10,000 times slower than in it does air (Sculthorpe, 1967; Leyton, 1975). These restrictions significantly retard O_2 uptake, especially under stagnant conditions when thick boundary layers develop (Sculthorpe, 1967; Westlake, 1967). Therefore, O_2 availability for submersed plants is likely, at least on a diurnal basis, to be in limited supply (Smith et al., 1984; Smith et al., 1988). It seems reasonable then, to expect that submersed plants have adapted to reduced sediments in a manner which is conservative with respect to O_2. One possible adaptation would be to increase O_2 availability by increasing the

porosity and hence lacunar storage capacity of the plant body. This does not appear to be an adaptation found among submersed plants, however, since the results of this study show that, on a cross-sectional basis, species which typically root in sediments with high O_2 demands are characterized by tissues of low porosity.

Porosity values differed significantly among the species examined. Decreasing porosity was found to be directly related to an increase in resistance to diffusion and a decrease in the plants ability to transport O_2 to the roots. The differences in porosity observed between species were evaluated and considered to be of physiological importance. Under the same conditions, species with low diffusive resistances should be able to transport more O_2 to the roots than species with high diffusive resistances. If O_2 transport occurs primarily by diffusion, these results also suggest that species with higher porosity or low diffusive resistance should be able to support a larger rooting biomass than species with lower porosity values. This trend was observed among the species examined. Decreasing porosity was found to be correlated with an increase in the resistance to diffusion and a decrease in relative root production.

A decrease in the amount of roots a plant produces should, due to a decrease in the volume of tissue, reduce the total amount of O_2 required for respiration (Williams and Barber, 1967) and should also, due to decrease in the surface area, reduce the amount of O_2 released from the root. These features would lead to a reduction in the total amount of O_2 required for transport. Suberin deposits in the cell wall of hypodermal cells may restrict the amount of O_2 released across the roots. This would restrict release of O_2 from the roots and promote diffusion of O_2 down the root to the root tip where it is especially needed for growth and development.

This discussion leads to the following model for the distribution of submersed plants within lakes. In this model, relative root production and porosity are plotted against sediment O_2 demand (Figure 86). Typically within lakes, release of nutrients from the sediments to the overlying water increases as the O_2 demand of the sediment increases (Wetzel, 1975). As the concentration of nutrients in the water increases, the productivity of phytoplankton also increases which can result in a decrease in light penetration (Wetzel, 1975). Therefore along a gradient of increasing O_2 demand, one would expect to find an increasing concentration of nutrients in the water and an increase in the extinction coefficient for light penetration. The results of this study suggest that species distributed along this gradient will be characterized by a decrease in the relative amount of roots produced as well as a decrease in the porosity of the plant body.

Lobelia is typically found in nutrient poor sediments with low O_2 demands (Moyle, 1945; Seddon, 1972). It produces an abundant root supply by which it obtains nutrients (Moeller, 1978). In these sediments, *Lobelia* releases enough O_2 from its roots to maintain a fully oxidized rhizosphere (Wium-Andersen and Andersen, 1972). It is characterized by a short rosette growth form, yet may receive enough light for photosynthesis due to the high penetration of light in these oligotrophic environments. The high O_2 storage potential of this species may be due to a large lacunar volume and a thick cuticle across the leaves which restricts the release of O_2. The lacunar system provides a short and continuous pathway and therefore should also facilitate the transport of O_2 from the leaves to the roots. *Lobelia* is unable, however, to transport enough O_2 to the roots to exist in more organic sediments characterized by higher O_2 demands (Moyle, 1945; Farmer and Spence, 1986). Features which promote O_2 storage may also

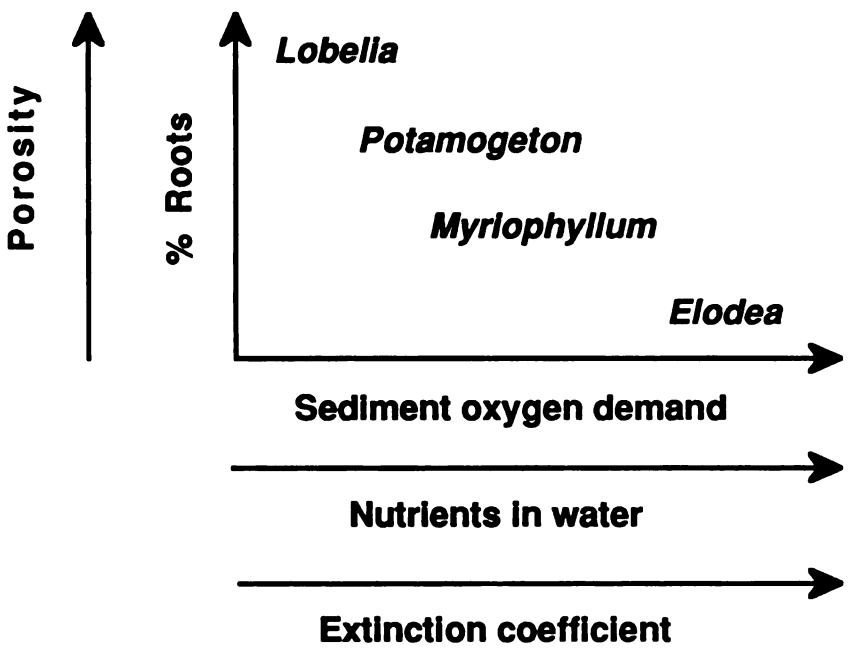

Figure 86. Model of distribution of submersed plants within lakes.

restrict O_2 uptake during the dark and thus limit the amount of O_2 available for transport to that stored within the lacunar system during the day. This supply may be inadequate when the O_2 demand around the roots increases. In this species, both nutrient uptake and gas exchange would be expected to occur primarily across the roots and very little across the leaves.

Elodea, on the other hand, is commonly found in eutrophic lakes, where it often forms large floating mats (Sculthorpe, 1967). This growth form is likely to be adaptive for photosynthesis, since light is rapidly attenuated throughout the water column in these lakes. Eutrophic lakes are nutrient rich systems. The sediment O_2 demand is very high and nutrients are abundant in both the sediment and in the overlying water (Wetzel, 1975). Since this species produces very few roots, nutrient uptake across the leaves would be expected to predominate. Decreasing the amount of roots buried in these sediments reduces the amount of O_2 required for transport. An efficient transport system, one characterized by low resistance to diffusion for example, may not be required to support this small rooting biomass. Features such as thin leaves, thin cuticles and small lacunar volumes may enhance the release of O_2 across the leaves. These features should facilitate not only the uptake of O_2 and CO_2 from the water column but also the uptake of nutrients across the leaves. Thus in *Elodea*, most of the gas exchange and nutrient uptake would be expected to occur across the leaves and very little across the roots.

Species such as *Potamogeton* and *Myriophyllum* are intermediate between *Lobelia* and *Elodea* with respect to these characteristics. Stems of *Potamogeton* were more porous than stems of the *Myriophyllum* species examined. These results suggest that, due to a lower diffusive resistance, *Potamogeton* would be able to support a larger rooting

biomass than *Myriophyllum*. Similarly differences in porosity between the *Myriophyllum* species would suggest that *M. spicatum* would be able to support a larger rooting system than *M. heterophyllum*. These results, however, could also be interpreted that, at a given root biomass, M. spicatum would be expected to transport more O_2 to the roots than *M. heterophyllum* and therefore should be able to root in sediments with higher O_2 demands. The physiological/ecological significance of these findings should be examined further.

The ability of emergent aquatic plants to transport and release O_2 from their roots appears to be directly related to their distribution; plants with high rates of O_2 release are able to root in sediments with high O_2 demands (Armstrong, 1964; 2979; Yamasaki, 19876). This relationship does not appear to directly apply to submersed plants. The results of this study suggest the inverse. Plants with high diffusive transport abilities are characterized by large rooting systems which are buried in sediments of low O_2 demand. Plants with low O_2 diffusive transport abilities are characterized by small rooting systems and are typical of lakes with high O_2 sediment demands.

The O_2 concentration within the lacunar system of submersed plants varies throughout the day and is highly dependent upon the photosynthetic rate of the plant. The results of this study showed that a steep O_2 gradient between the shoots and the roots, as is typically found during active photosynthesis, may be sufficient, by diffusion alone, to satisfy the O_2 demands of the roots. During the night or during periods of low photosynthesis, the O_2 gradient is likely to be too small to support this rate of O_2 transport. This suggests that environmental factors, such as changes in light intensity, will also affect the ability of submersed plants to transport O_2 to the roots. Therefore, the photosynthetic rate of the plant may determine not only the availability of

carbohydrates for root growth, but also the availability of O_2 for root respiration and release to the sediments.

LIST OF REFERENCES

LIST OF REFERENCES

Adams, M.S. and K.D. McCracken. 1974. Seasonal production of the *Myriophyllum* component of the littoral of Lake Wingra, Wisconsin. J. Ecol. 62:457-465.

Arber, A. 1920. Water plants. Cambridge University Press, Cambridge. 436 pp.

Armstrong, W. 1964. Oxygen diffusion from the roots of some British bog plants. Nature, Lond. 204:801-802.

Armstrong, W. 1972. A re-examination of the functional significance of aerenchyma. Physiol. Plant. 27:173-177.

Armstrong, W. 1971. Radial oxygen losses from intact rice roots as affected by distance from the apex, respiration and waterlogging. Physiol. Plant. 25:192-197.

Armstrong, W. 1979. Aeration in higher plants. In: Advances in botanical research, Vol. 7, H.W. Woolhouse (Ed.). Academic Press, London. pp. 226-332.

Armstrong, W. 1982. Waterlogged soils. In: Environment and plant ecology. J.R. Etherington (Ed.). John Wiley, Chicester. pp. 209-332.

Armstrong, J. and W. Armstrong. 1988. *Phragmites australis*- A preliminary study of soil-oxidizing sites and internal gas transport pathways. New Phytol. 108:373-382.

Armstrong, J. and W. Armstrong. 1990. A convective through-flow of gases in *Phragmites australis*. Aquat. Bot (in press).

Armstrong, J., W. Armstrong and P.M. Beckett. 1988. *Phragmites australis*: a critical appraisal of the ventilating pressure concept and an analysis of resistance to pressurized gas flow and gaseous diffusion in horizontal rhizomes. New Phytol. 110:383-389.

Barber, D.A. 1961. Gas exchange between Equisetum limnosum and its environment. J. Exp. Bot. 12:243-251.

Barber, D.A., M. Ebert and N.T.S. Evans. 1962. The movement of ^{15}O through barley and rice plants. J. Exp. Bot. 397-403.

Barko, J. W. 1983. The growth of *Myriophyllum spicatum* L. in relation to selected characteristics of sediment and solution. Aquatic. Bot. 15:91-103.

Barko, J.W. and R.M. Smart. 1983. Effects of organic matter additions to sediment on the growth of aquatic plants. J. Ecol. 71: 161-175.

Barnabas, A.D. 1982. Fine structure of the leaf epidermis of *Thalassodendron ciliatum* (Forsk.) den Hartog. Aquat. Bot. 12:41-55.

Barnabas, A.D., V. Bulter and T.D. Steinke. 1977. *Zostera capensis* Setchell: Observations on the fine structure of the leaf epidermis. Z. Pflanzenphysiol. 85:417-427.

Barnabas, A.D., V. Butler and T.D. Steinke. 1980. *Zostera capensis* Setchell II. Fine structure of the cavities in the wall of leaf blade epidermal cells. Z. Pflanzenphysiol. Bd. 99:95-103.

Bartlett, R.J. 1961. Iron oxidation proximate to plant roots. Soil Sci. 92:372-379.

Beckett, P.M., W. Armstrong, S.H.F.W. Justin and J. Armstrong. 1988. On the relative importance of convective and diffusive gas-flows in plant aeration. New Phytol. 110:463-469.

Benedict, C.R. and J.R. Scott. 1976. Photosynthetic carbon metabolism of a marine seagrass. Plant Physiol. 57:876-880.

Birch, W.R. 1974. The unusual epidermis of the marine angiosperm *Halophila* Thou. Flora, Bd. 163:410-414.

Black, M.A., S.C. Maberly and D.H.N. Spence. 1981. Resistance to carbon dioxide fixation in four submerged freshwater macrophytes. New Phytol. 89:557-568.

Borutuskii, E.V. 1950. (Data on the dynamics of the biomass of the macrophytes of lakes. In Russian). Trudy vses. gidrobiol. Obshc. 2:43-66.

Boston, H.L., M.S. Adams and T.P. Pienkowski. 1987. Utilization of sediment CO_2 by selected North American isoetids. Ann. Bot. 60:485-494.

Boston, H.L., M.S. Adams and T.P. Pienkowski. 1987. Models of the use of root-zone CO_2 by selected North American isoetids. Ann. Bot. 60:495-503.

Boynton, W.P. and W.H. Brattain. 1929. Interdiffusion of gases and vapors. In: International critical tables of numerical data. Physics, Chemistry and Technology. Vol V. E.W. Washburn (Ed.). McGraw-Hill, London. pp. 62-63.

Bristow, J.M. 1975. The structure and function of roots in aquatic vascular plants. In: The development and function of roots. J.G. Torrey and D.T. Clarkson (Eds). Academic Press, New York. pp. 221-236.

Brix, H. 1988. Light-dependent variations in the composition of the internal atmosphere of *Phragmites australis* (Cav.) Trin. ex Steudel. Aquat. Bot. 30:319-329.

Brix, H. 1989. Gas exchange through dead culms of reed, *Phragmites australis* (Cav.) Trin. ex Stuedel. Aquat. Bot. 35:81-98.

Browse, J.A., F.I. Dromgoole and J.M.A. Brown. 1977. Photosynthesis in the aquatic macrophyte *Egeria densa*. I. $^{14}CO_2$ fixation at natural CO_2 concentrations. Aust. J. Plant Physiol. 6:1-9.

Browse, J.A., F.I. Dromgoole and J.M.A. Brown. 1979. Photosynthesis in the aquatic macrophyte *Egeria densa*. III. Gas exchange studies. Aust. J. Plant Physiol. 6:499-512.

Cambridge, M.L. and J. Kuo. 1982. Morphology, anatomy and histochemistry of the Australian seagrasses of the genus *Posidonia* Konig (Posidoniaceae). III. Posidonia sinuosa Cambridge & Kuo. Aquat. Bot. 14:1-14.

Carpenter, S.R., J.J. Elser, and K.M. Olson. 1983. Effects of roots of *Myriophyllum verticillatum* L. on sediment redox conditions. Aquat. Bot. 17:243-249.

Chafe, S.C. 1970. The fine structure of the collenchyma cell wall. Planta 90:12-21.

Chafe, S.C. and A.B. Wardrop. 1972. Fine structural observations on the epidermis. I. The epidermal cell wall. Planta 107:269-278.

Chambers, P.A. and J. Kalff. 1985. The influence of sediment and irradiance on the growth and morphology of *Myriophyllum spicatum* L. Aquat. Bot. 22:253-263.

Chen, C.C., J.B. Dixon and F.T. Turner. 1980. Iron coatings on rice roots: mineralogy and quantity influencing factors. Soil Sci. Soc. Am. J. 44:635-639.

Clarkson, D.T., A.W. Robards, J. Sanderson and C.A. Peterson. 1978. Permeablitly studies on epidermal-hypodermal sleeves isolated from roots of *Allium cepa* (onion). Can. J. Bot. 56:1526-1532.

Clarkson, D.T., A.W. Robards, J.E. Stephens and M. Stark. 1987. Suberin lamellae in the hypodermis of maize (*Zea mays*) roots; development and factors affecting the permeablility of hypodermal layers. Plant, Cell and Environment 10:83-93.

Coult, D.A. 1964. Observations on gas movement in the rhizome of *Menyanthes trifoliata* L., with comments on the role of the endodermis. J. Exp. Bot. 15:205-218.

Cormack, R.G.H. 1937. The development of root hairs by *Elodea canadensis*. New Phytol. 36:19-25.

Crawford, R.M.M. 1978. Metabolic adaptations to anoxia. In: Plant life in anaerobic environments. D.D. Hook and R.M.M. Crawford (Eds.) Ann Arbor Science Publishers, Inc., Ann Arbor. pp. 119-136.

Crow, E.G. and C.B. Hellquist. 1983. Aquatic vascular plants of New England. Part 6: Haloragaceae. New Hampshire Ag. Exp. Station, Univer. New Hampshire, Durham. Station Bulletin 524, 26 pp.

Dacey, J.W.H. 1980. Internal winds in waterlilies: an adaptation for life in anaerobic environments. Science 210:1017-1019.

Dacey, J.W.H. 1981. Pressurized ventilation in the yellow waterlily. Ecology 62:1137-1147.

Dacey, J.W.H. 1987. Knudsen-transitional flow and gas pressurizaiton in leaves of *Nelumbo*. Plant Physiol. 85:199-203.

Dacey, J.W.H. and M.J. Klug. 1979. Methane efflux from lake sediments through waterlilies. Science 203:1253-1255.

Dale, H.M. 1957. Developmental studies of *Elodea canadensis* Michx. I. Morphological development of the shoot apex. Can. J. Bot. 35:13-24.

Dale, H.M. 1957. Developmental studies of *Elodea canadensis* Michx. II. Experimental studies on morphological effects of darkness. Can. J. Bot. 35:51-64.

Denny, P. 1980. Solute movement in submerged angiosperms. Biol. Rev. 55:65-92.

Doohan, M.E. and E.H. Newcomb. 1976. Leaf ultrastructure and $\delta^{13}C$ values of three seagrasses from the Great Barrier Reef. Aust. J. Plant Physiol. 3:9-23.

Drew, M.C. and J.M. Lynch. 1980. Soil anaerobiosis, microorganisms, and root function. Ann. Rev. Phytopathol. 18:37-66.

Falk, H. and P. Sitte. 1963. Zellfeinbau bei Plasmolyse. I. Der Feinbau der *Elodea* Blattzellin. Protoplasma 57:290-303.

Farmer, A.M. and D.H.N. Spence. 1986. The growth strategies and distribution of isoetids in Scottish freshwater lochs. Aquat. Bot. 26:247-258.

Feder, N. and T.P. O'Brein. 1968. Plant microtechnique: some principles and new methods. Am. J. Bot. 55:123-142.

Ferguson, I.B. and D.T. Clarkson. 1976. Ion uptake in relation to the development of a root hypodermis. New Phytol. 77:11-14.

Gill, J.L. 1978. Design and analysis of experiments in the animal and medical sciences. Iowa State University Press, Iowa. 409 pp.

Grace, J.B. and R.G. Wetzel. 1978. The production biology of Eurasion watermilfoil (*Myriophyllum spicatum* L.): a review. J. Aquat. Plant Manage. 16:1-11.

Green, M.S. and J.R. Etherington. 1977. Oxidation of ferrous iron by rice (Oryza sativa L.) roots: a mechanism for waterlogging tolerance? J. Exp. Bot. 28:678-690.

Gunning, E.S. and J.S. Pate. 1969. "Transfer cells"- plant cells with wall ingrowths, specialized in relation to short distance transport of solutes- their occurence, structure, and development. Protoplasma 68:107-133.

Hasman, M. and N. Inanc. 1957. Investigations on the anatomical structure of certain submerged, floating and amphibious hydrophytes. Instanb. Univ. Fen Fak. Mecm., ser. B. 22:137-153.

Hartman, R.T. and D.L. Brown. 1967. Changes in the internal atmosphere of submerged vascular hydrophytes in relation to photosynthesis. Ecology 48:252-258.

Holloway, P.J. 1982. Structure and histochemistry of plant cuticular membranes: an overview. In: The Plant Cuticle. D.F. Cutler, K.L. Alvin and C.E. Price (Eds). pp. 1-32. Academic Press, London. 461 pp.

Hough, R.A. 1974. Photorespiration and productivity in submersed aquatic vascular plants. Limnol. Oceanogr. 19:912-927.

Hough, R.A. and R.G. Wetzel. 1977. Photosynthetic pathways of some aquatic plants. Aquat. Bot. 3:297-313.

Howard-Williams, C., B.R. Davies and R.H.M. Cross. 1978. The influence of periphyton on the surface structure of a *Potamogeton pectinatus* L. leaf (an hypothesis). Aquat. Bot. 5:87-91.

Hutchinson, G.E. 1975. A treatise on limnology. Vol III. Limnological botany. John Wiley & Sons, New York. 660 pp.

Jagels, R. 1973. Studies of a marine grass, *Thalassia testudinum*. I. Ultrastructure of the osmoregulatory leaf cells. Am. J. Bot. 60:1003-1009.

Johansen, D.A. 1940. Plant microtechnique. McGraw-Hill, New York.

Justin, S.H.F.W. and W. Armstrong. 1983. Oxygen transport in the salt marsh genus *Puccinella* with particular reference to the diffusive resistance of the root-shoot junction and the use of paraffin oil as a diffusive barrier in plant studies. J. Exp. Bot. 34:980-986.

Kawase, M. 1981. Anatomical and morphological adaptation of plants to waterlogging. Hortscience 16:30-34.

Kemp, W.M. and L. Murray. 1986. Oxygen release from roots of the submersed macrophyte *Potamogeton perfoliatus* L.: regulating factors and ecological implications. Aquat. Bot. 26:271-283.

Koncalova, H., J. Pokorny and J. Kvet. 1988. Root ventilation in *Carex gracilis* Curt.: diffusion or mass flow? Aquat. Bot. 30:149-155.

Kuo, J. 1978. Morphology, anatomy and histochemistry of the Australian seagrasses of the genus *Posidonia* Konig (Posidoniaceae). I. Leaf blade and leaf sheath of *Posidonia australis* Hook. f. Aquat. Bot. 5:171-190.

Kuo, J. and M.L. Cambridge. 1978. Morphology, anatomy and histochemistry of the Australian seagrasses of the genus *Posidonia* Konig (Posidoniaceae). II. Rhizome and root of *Posidonia australis* Hook. f. Aquat. Bot. 5:191-206.

Leyton, L. 1975. Fluid behavior in biological systems. Oxford University Press, Oxford. 235 pp.

Lunney, C.A., G.J. Davis and M.N. Jones. 1975. Unusual structures associated with peripheral reticulum in chloroplasts of *Myriophyllum spicatum* L. J. Ultrastruct. Res. 50:293-296.

Madsen, T.V. and M. Søndergaard. 1983. The effects of current velocity on the photosynthesis of *Callitriche stagnalis* Scop. Aquat. Bot. 15:187-193.

Mahlberg, P. 1972. Further observations on the phenomena of secondary vacuolation in living cells. Am. J. Bot. 59:172-179.

Mendelssohn, I.A. and M.T. Postek. 1982. Elemental analysis of deposits on the roots of *Spartina alterniflora* Loisel. Am. J. Bot. 69:904-912.

Moeller, R.E. 1978. Seasonal changes in biomass, tissue chemistry and net production of the evergreen hydrophyte, *Lobelia dortmanna*. Can. J. Bot. 56:1425-1433.

Mollenhauer, H.H. 1964. Plastic embedding mixtures for use in electron microscopy. Stain Technol. 39:111-114.

Moyle, J.B. 1945. Some chemical factors influencing the distribtuion of aquatic plants in Minnesota. Am. Midl. Natur. 34:402-420.

Nicholson, S.A. and D.G. Best. 1974. Root:shoot and leaf area relationships of macrophyte communities in Chautauqua Lake, New York. Bull. Torrey Bot. Club 101:96-100.

Nobel, P.S. 1983. Biophysical plant physiology and ecology. Freeman, San Francisco, CA. 608 pp.

Oremland, H.T. and B.F. Taylor. 1977. Diurnal fluctuations of O_2, N_2 and CH_4 in the rhizosphere of *Thalassia testudinum*. Limnol. Oceanogr., 22:566-570.

Ozimek, T., A. Prejs and K. Prejs. 1976. Biomass and distribution of underground parts of *Potmogeton perfoliatus* L. and *P. lucens* L. in Mikoljskie Lake, Poland. Aquat. Bot. 2:309-316.

Payne, F.C. 1982. Influence of hydrostatic pressure on gas balance and lacunar structure in *Myriophyllum spicatum* L. Ph.D. Dissertation, Michigan State Univ. 109 pp.

Penhale, P.A. and R.G. Wetzel. 1983. Structural and functional adaptations of eelgrass (*Zostera marina* L.) to the anaerobic sediment environment. Can. J. Bot., 61:1471-1478.

Pendland, J. 1979. Ultrastructural characteristics of *Hydrilla* leaf tissue. Tissue and Cell 11:79-88.

Peterson, C.A., R.L. Peterson and A.W. Robards. 1978. A correlated histochemical and ultrastructural study of the epidermis and hypodermis of onion roots. Protoplasma 96:1-21.

Ponnamperuma, F.N. 1984. Effects of flooding on soils. In: Flooding and plant growth. T.T. Kozlowski (Ed). Academic Press Inc., Orlando. pp. 10-45.

Raskin, I. and H. Kende. 1983. How does deep-water rice solve its aeration problem? Plant Physiol. 72:447-454.

Raskin, I. and H. Kende. 1985. Mechanism of aeration in rice. Science 228:327-329.

Reynolds, E.S. 1963. The use of lead citrate of high pH as an electron opaque stain in electron microscopy. J. Cell Biol. 17:208-212.

Rich, P., R.G. Wetzel and N.V. Thuy. 1971. Distribution, production and role of aquatic macrophytes in a southern Michigan marl lake. Freshwat. Biol. 1:8-21.

Robards, A.W. D.T. Clarkson and J. Sanderson. 1979. Structure and permeablility of the epidermal/hypodermal layers of the sand sedge (*Carex arenaria* L.). Protoplasma 101:331-347.

Robb, F., B.R. Davies, R. Cross, C. Kenyon and C. Howard-Williams. 1979. Cellulolytic bacteria as primary colonizers of *Potamogeton pectinatus* (Sago pond weed) from a brackish south-temperate coastal lake. Microb. Ecol. 5:167-177.

Roberts, D.G., A.J. McComb and J. Kuo. 1984. The structure and continuity of the lacunar system of the seagrass *Halophila ovalis* (R.Br.) Hook f. (Hydrocharitaceae). Aquat. Bot. 18:377-388.

Roberts, D.G. and D.J.W. Moriarty. 1987. Lacunal gas discharge as a measure of productivity in the seagrasses, *Zostera capricorni*, *Cymodocea serrulata* and *Syringodium isoetifolium*. Aquat. Bot. 28:143-160.

Rogers, K.H. and C.M. Breen. 1981. Effect of epiphyton on *Potamogeton crispus* L. leaves. Microb. Ecol. 7:351-363.

Sand-Jensen, K. 1983. Photosynthetic carbon sources of stream macrophytes. J. Exp. Bot. 34:198-210.

Sand-Jensen, K. and C. Prahl. 1982. Oxygen exchange with the lacunae and across leaves and roots of the submerged vascular macrophyte, *Lobelia dortmanna* L. New Phytol. 91:103-120.

Sand-Jensen, K., C. Prahl and H. Stockholm. 1982. Oxygen release from roots of submerged aquatic macrophytes. Oikos 38:349-354.

Sanderson, P.L. and W. Armstrong. 1978. Soil waterlogging, root rot and conifer windthrow: oxygen deficiency or phytotoxicity? Plant Soil 49:185-190.

Schönherr, J. 1976. Water permeability of isolated cuticular membranes. The effect of cuticular waxes on diffusion of water. Planta 131:159-164.

Schröder, P, W. Grosse and Woermann. 1986. Localization of thermo-osmotically active partitions in young leaves of *Nuphar lutea*. J. Exp. Bot. 37:1450-1461.

Sculthorpe, C.D. 1967. The biology of aquatic vascular plants. Edward Arnold, London. 610 pp.

Seddon, B. 1972. Aquatic macrophytes as limnological indicators. Freshwat. Biol. 2:107-130.

Shannon, E.L. 1953. The production of root hairs by aquatic plants. Am. Midland Nat. 50:474-479.

Sharpe, V. and P. Denny. 1976. Electron microscope studies on the absorption and localization of lead in the leaf tissue of *Potamogeton pectinatus* L. J. Exp. Bot. 27:1155-1162.

Sitte, P. 1963. Zellfeinbau bei Plasmolyse. II. Der Feinbau der *Elodea* Blattzellen bei Zucker and Ionenplasmolyse. Protoplasma 57:304-333.

Smith, F.A. and N.A. Walker. 1980. Photosynthesis by aquatic plants: effects of unstirred layers in relation to assimilation of CO_2 and HCO_3 and to carbon isotope discrimination. New Phytol. 86:245-259.

Smith, R.D., W.C. Dennison and R.S. Alberte. 1984. Role of seagrass photosynthesis in root aerobic processes. Plant Physiol. 74:1055-1058.

Smith, R.D., A.M. Pregnall and R.S. Alberte. 1988. Effects of anaerobiosis on root metabolism of *Zostera marina* (eelgrass); implications for survival in reducing sediments. Mar. Biol. 98:131-141.

Søndergaard, M. 1979. Light and dark respiration and the effect of the lacunal system on refixation of CO_2 in submerged aquatic plants. Aquat. Bot. 6:269-283.

Søndergaard, M. and S. Laegaard. 1977. Vesicular-arbuscular mycorrhiza in some aquatic vascular plants. Nature 268:232-233.

Søndergaard, M. and K. Sand-Jensen. 1979. Carbon uptake by leaves and roots of *Litorella uniflora* (L.) Aschers. Aquat. Bot. 6:1-12.

Søndergaard, M. and R. Wetzel. 1980. Photorespiration and internal recycling of CO_2 in the submerged angiosperm *Scirpus subterminalis*. Can. J. Bot. 58:591-598.

Sorrell, B.K. and F.I. Dromgoole. 1986. Errors in measurements of aquatic macrophyte gas exchange due to oxygen storage in internal airspaces. Aquat. Bot. 24:103-114.

Sorrell, B.K. and F.I. Dromgoole. 1987. Oxygen transport in the submerged freshwater macrophyte *Egeria densa* Planch. I. Oxygen production, storage and release. Aquat. Bot., 28:63-80.

Sorrell, B.K. and F.I. Dromgoole. 1988. Oxygen transport in the submerged freshwater macrophyte *Egeria densa* Planch. II. Role of lacunar gas pressures. Aquat. Bot. 31:93-106.

Spence, D.H.N. and J. Chrystal. 1970. Photosynthesis and zonation of freshwater macrophytes. I. Depth distribtuion and shade tolerance. New Phytol. 69:205-215.

Spurr, A.R. 1969. A low-viscosity epoxy resin embedding medium for electron microscopy. J. Ultrastruct. Res. 26:31-34.

Teal, J.M. and J.W. Kanwisher. 1966. Gas transport in the marsh grass *Spartina alterniflora*. J. Exp. Bot. 17:355-361.

Taylor, G.J., A.A. Crowder and R. Rodden. 1984. Formation and morphology of an iron plaque on the roots of *Typha latifolia* L. grown in solution culture. Amer. J. Bot. 71:666-675.

Thursby, G.B. 1984. Root-exuded oxygen in the aquatic angiosperm *Ruppia maritima*. Mar. Ecol. Prog. Ser. 16:303-361.

Tomlinson, P.B. 1969. On the morphology and anatomy of turtle grass, *Thalassia testudinum* (Hydrocharitaceae). II. Anatomy and development of the root in relation to function. Bull. Mar. Sci. 19:57-71.

Ting, I.P. 1982. Plant physiology. Addison-Wesley Pub. Reading, Mass. 597 pp.

Valanne, N., E.-M. Aro and E. Rintamaki. 1982. Leaf and chloroplast structure of two aquatic *Ranunculus* species. Aquat. Bot. 12:13-22.

Weisner, S.E.B. and W. Graneli. 1989. Influence of substrate conditions of the growth of *Phragmites australis* after a reduction in oxygen transport to below-ground parts. Aquat. Bot. 35:71-80.

Westlake, D.F. 1965. Some basic data for investigations of the productivity of aquatic macrophytes. Mem. Ist. Ital. Idrobiol. Suppl. 18:229-248.

Westlake, D.F. 1967. Some effects of low-velocity currents on the metabolism of aquatic macrophytes. J. Exp. Bot. 18:187-205.

Wetzel, R.G. 1975. Limnology. Saunders, Philadelphia, PA. 743 pp.

Wetzel, R.G., E.S. Brammer, K. Lundstrom and C. Forsberg. 1985. Photosynthesis of submersed macrophytes in acidified lakes. II. Carbon limitation and utilization of benthic CO_2 sources. Aquat. Bot. 22:107-120.

Williams, W.T. and D.A. Barber. 1961. The functional significance of aerenchyma in plants. Symp. Soc. Exp. Biol. 15:132-144.

Wium-Andersen, S. 1971. Photosynthetic uptake of free CO_2 by the roots of *Lobelia dortmanna*. Physiol. Plant. 25:245-248.

Wium-Andersen, S. and J.M. Andersen. 1972. The influence of vegetation on the redox profile of the sediment of Grane Langsø, a Danish *Lobelia* lake. Limnol. Oceanogr. 17:948-952.

Yamasaki, S. 1987. Oxygen demand and supply in Zizania latifolia and *Phragmites australis*. Aquat. Bot. 29:205-215.

Yamasaki, S. and T. Saeki. 1979. The effects of oxygen supply from the shoot on *Zizania latifolia* growth. Jpn. J. Ecol. 29:249-256.

APPENDICES

APPENDIX I

Standard Curve

A standard curve of 1/%transported versus resistance was constructed (Materials and Methods) and used to measure the resistance of stem tissue to the diffusion of CH_4 (Figure AI.1). The resistances of capillary tubing inserts were determined using Fick's first law, R=L/DA (Chapter IV), where L is the length and A is the cross-sectional gas space area of the tubing. D, the diffusion coefficient of CH_4 in air, was estimated from data reported by Boynton and Brattain (1929)(D=.20 cm2 s^{-1}, estimated). Resistance values employed ranged from 130-16800 s cm^{-3}. The regression was highly significant ($P<.0001$, $r^2=.92$, n=135).

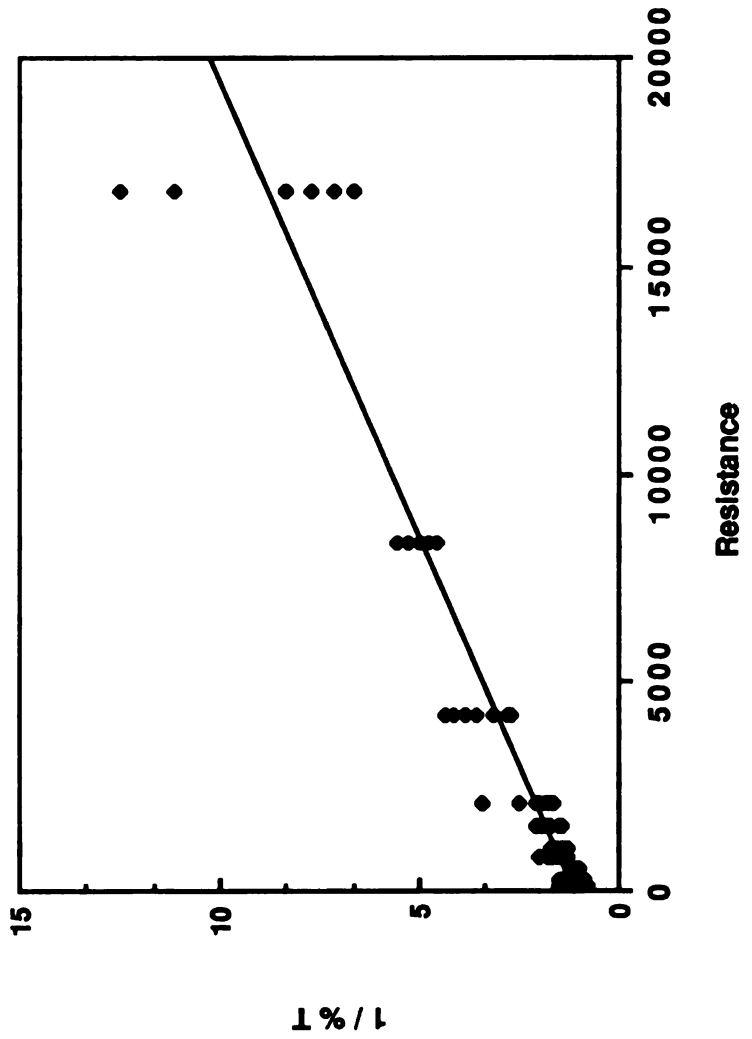

Figure AI.1. Standard curve used to estimate resistance to diffusion. Graph of 1/% Transported (T) versus resistance (s cm^{-3}). The solid line is a regression through data points. Resistance = (1/%T-1.06)/4.95×10^{-4}. (r^2=.92, n=135).

APPENDIX II

Predicted Estimates of Resistance

Estimates of internodal resistance to both diffusion and mass flow were based on anatomical observations of porosity, lacunar area and lacunar number from fresh tissue. Lacunar diameter was estimated from the mean lacunar area. These estimates and predicted estimates of resistance are presented in Table AII.1.

Estimates of nodal resistance to both diffusion and mass flow were based on anatomical observations of pore size and frequency from SEM photographs taken of nodes that were fixed, dehydrated and critical point-dried. A study was conducted to examine the effects of this procedure on the dimensions of these features. Cross-sections of fresh stem tissue of *Potamogeton* were compared with processed tissues taken from the same stem sections and were examined for porosity, mean pore area and number of pores per node. Pore diameter was determined from the mean pore area. Processing of stems resulted in a 26% $\pm$ 6% (95% confidence interval, n=9) shrinkage of the tissue. The data were adjusted to account for shrinkage (Table AII.2). Predicted estimates of nodal resistance were calculated using these adjusted values (Table AII.2).

Table AII.1. Anatomical characteristics of stems. Values used in calculation of internodal resistance to diffusion (R_I, s cm^{-3}) and mass flow (r_i, kPa s cm^{-3}) for four species. Data are presented as mean ± 95% confidence interval (n usually > 20).

Species	Stem diameter (cm)	Lacunar radius	# Lacunae $stem^{-1}$	Porosity	Gasspace	R_I	r_I
M. spicatum	.16	.017 ± .003	13 ± 1	.498 ± .013	.012 ± .001	416 ± 25	.13
	.20	.021 ± .003	13 ± 1	.522 ± .015	.018 ± .001	303 ± 29	.02
M. heterophyllum	.20	.015 ± .001	19 ± 1	.346 ± .009	.011 ± .001	441 ± 35	.05
Potamogeton	.24	.010 ± .001	123 ± 6	.658 ± .026	.039 ± .001	132 ± 6	.04
Elodea	.12	.004 ± .001	58 ± 19	.248 ± .029	.003 ± .001	1931 ± 256	3.14

Table AII.2. Morphological and anatomical characteristics of nodes/diaphragms. Values used in calculation of nodal resistance to diffusion (R_n, s cm^{-3}) and mass flow (r_n, kPa s cm^{-3}) for four species. Data are presented as mean ± 95% confidence interval.

Species	Stem diameter (cm)	# pores cm^{-2}	# pores node $^{-1}$	pore length (cm)	mean pore diameter (cm)	porosity	R_n	r_n	n
M. spicatum	.16	194,441 ± 65,772	2287 ± 1011	$1.3x10^{-3}$ ± $8x10^{-5}$	$2.9x10^{-4}$ ± $3x10^{-5}$	.017 ± .006	72 ± 40	64 ± 37	9
	.20	288,079 ± 22,459	4205 ± 250	$1.6x10^{-3}$ ± $1x10^{-4}$	$5.1x10^{-4}$ ± $7x10^{-5}$	.076 ± .013	13 ± 3	6 ± 3	9
M. heterophyllum	.20	391,733 ±110,418	4092 ± 1140	$1.4x10^{-3}$ ± $1x10^{-4}$	$3.2x10^{-4}$ ± $1x10^{-5}$	.066 ± .018	36 ± 26	55 ± 68	6
Potamogeton	.24	423,315 ± 35,968	15175 ± 1340	$7.0x10^{-4}$ ± $2x10^{-5}$	$2.7x10^{-4}$ ± $2x10^{-5}$	.093 ± .018	6 ± 1	8 ± 3	9
Elodea	.12	84,761 ± 13,807	233 ± 38	$1.8x10^{-3}$ ±$1.2x10^{-4}$	$6.2x10^{-4}$ ± $7x10^{-4}$	.032 ± .007	66 ± 42	51 ± 29	9

APPENDIX III

Transport Studies in Potamogeton illinoensis

In the flow-through system of waterlilies, a pressure differential is established between young pressurized leaves and old leaves which serve as vents (Dacey, 1980; 1981). *Potamogeton illinoensis* was chosen for study to demonstrate the potential for mass flow in submersed plants. This rhizotomatous plant produces a small spike of emergent flowers. It was hypothesized that these flowers may provide a means of venting pressures which may build up in the plant during photosynthesis. If a pressure differential develops between submersed stems and stems with emergent flowers, then one would expect a mass flow of gases down the submersed stem, through the rhizome and out stems with emergent flowers.

As gases flow through the rhizome of waterlilies they become enriched in CH_4 which diffuses into the rhizome from the sediments (Dacey and Klug, 1978). Flowers of *P. illinoensis* were bagged and sampled for CH_4 over a 24 hour period (Dacey and Klug, 1978). The CH_4 concentration increased considerably during the photosynthetic period in some bags, while in others CH_4 levels remained relatively low. The results were confusing at the time until stems were examined carefully. Chironomid larvae bury into these stems and eventually flood the lacunar system. Flooding blocks the pathway to

both diffusion (n=11) and mass flow (n=11). It may be possible that stems with flowers that did not release CH_4 were infected with these larvae. If the lacunar system were flooded, CH_4 could not be transported up from the rhizome and released from the flower. If this explanation is correct, then release of CH_4 from the flowers only during the day would support the hypothesis of mass flow through these plants.

The effect of infestation by chironomid larvae on O_2 transport in submersed plants has not, to my knowledge, been examined. The results presented here suggest that stems infected with chironomid larvae may not be capable of transporting O_2 to roots and rhizomes. These insects may therefore have a significant impact of the physiology and ecology of the plants they infect.